



Ramírez-Torres, A., Di Stefano, S. and Grillo, A. (2021) Influence of non-local diffusion in avascular tumour growth. *Mathematics and Mechanics of Solids*, (doi: 10.1177/1081286520975086).

There may be differences between this version and the published version. You are advised to consult the publisher's version if you wish to cite from it.

<http://eprints.gla.ac.uk/232136/>

Deposited on: 18 March 2021

Enlighten – Research publications by members of the University of Glasgow  
<http://eprints.gla.ac.uk>

# Influence of non-local diffusion in avascular tumour growth

Ariel Ramírez-Torres<sup>1,2</sup>, Salvatore Di Stefano<sup>1</sup>, and Alfio Grillo<sup>1</sup>

<sup>1</sup>Dipartimento di Scienze Matematiche “G. L. Lagrange” Politecnico di Torino, 10129. Torino, Italia

<sup>2</sup>School of Mathematics and Statistics, Mathematics and Statistics Building, University of Glasgow, University Place, Glasgow G128QQ, UK

## Abstract

The availability and evolution of chemical agents play an important role in the growth of a tumour and, therefore, the mathematical description of their consumption is of special interest. Usually, Fick’s law of diffusion is adopted for describing the local character of the evolution of chemicals. However, in a highly complex, heterogeneous medium, as is a tumour, the progression of chemical species could be influenced by non-local interactions. In this respect, our goal is to investigate the influence of such type of diffusion on the growth of a tumour in avascular stage. For our purposes, we consider a diffusion equation for the evolution of the chemical agents that accounts for the existence of non-local interactions in a non-Fickian manner, and that involves notions of Fractional Calculus. In particular, the introduction of derivatives or integrals of fractional type of order  $\alpha \in \mathbb{R}$  has proven to be an effective mathematical tool in the description of various non-local phenomena. To achieve our goals, we adopt part of the modelling assumptions outlined in previous works of the authors, in which the growth of a tumour is described in terms of mass transfer among the tumour’s constituents and structural changes that occur in the tumour itself in response to growth. The latter ones are characterised by means of the Bilby–Kröner–Lee decomposition of the deformation gradient tensor. We perform numerical simulations, whose results indicate the relevance of embracing a fractional framework in modelling tumour growth. Specifically, the real parameter  $\alpha$  “dominates” the way in which the tumour grows, since it permits to model a variety of growth patterns ranging from the standard growth to no growth at all.

**Keywords** Tumour growth, non-Fickian diffusion, non-local interactions, inelastic distortions

# 1 Introduction

For several years now, the scientific literature has experienced an important increase in the mathematical modelling of tumour growth (see e.g. [20, 14, 8, 64, 100, 78, 7, 107, 66, 97, 65] and the references therein). However, there is still the necessity for understanding the connections among the different processes of chemical, biological and/or mechanical nature that take place at different time and length scales and influence the evolution of a tumour.

From the mechanical perspective, the growth of a tumour is closely related to the appearance of transformations of its internal structure that arise in response to mass changes, which may be driven by its chemo-mechanical environment and coexist with the visible deformation of the tumour itself [39, 32, 95]. A relevant aspect of this phenomenology is that the structural transformations are often accompanied by the production of residual stresses [98, 73, 52, 28, 101]. In this respect, we mention the series of experiments conducted by Stylianopoulos et al. [110] on tumour spheroids, which indicate the existence of an incompatible, stress-free state for such systems and, thus, suggest to interpret growth in terms of inelastic distortions in addition to mere changes of shape. This conclusion permits to invoke the Bilby–Kröner–Lee (BKL) multiplicative decomposition of the deformation gradient tensor [85, 52, 102]. As long as volumetric growth is concerned and, as in the case of the present work, no other types of structural transformations are accounted for, the BKL decomposition reduces to decomposing the deformation gradient tensor into two contributions. One is related to the changes of the tissue’s internal structure due to the gain or loss of mass, and the other one to distortions of purely elastic nature (note that, here and in the sequel, we shall use the terms “tumour” and “tissue” interchangeably). We refer to the works [102, 52, 94, 27, 101, 56], and to the references therein, for a more complete discussion on the BKL multiplicative decomposition.

It is worth noting that, although the inelastic distortions accompanying growth play an important role on its evolution [61, 6, 4, 51, 80], which may also be partially self-driven [41, 101], it is clear that the growth of a tumour is strongly conditioned by the presence of chemical agents of various nature, such as nutrients. Therefore, in order to elaborate a model of tumour growth, it is crucial to be able to model the evolution of chemical substances. Fick’s law of diffusion is largely adopted for this purpose, even though it has often turned out to be inconsistent with the results of some observed transport processes [48, 21, 31], which are thus referred to as *non-Fickean*. In fact, non-Fickean diffusion processes have been recognised in several biological tissues, including cells [48, 31], neuromuscular junctions [74] and brain tissue [21], among others. In particular, the experiments conducted by Danyuo et al. [34] suggest that cancer drug release kinetics in breast cancer is non-Fickean.

A common characteristic of the occurrence of non-Fickean patterns, as suggested in several works [70, 84, 48, 67, 45], is the multi-scale and heterogeneous nature of the environment in which diffusion takes place. Specifically, Lacks [74] shows that geometric factors, such as tortuosity, could cause the diffusion processes occurring in a neuromuscular junction to be non-Fickean. Within this view, in the case of a tumour, although to our knowledge there is no experimental evidence that correlates non-Fickean diffusion with its internal structure, its microvascular network is known to have a strong influence on transport phenomena. In fact, this issue has been discussed in several papers, like e.g. [69, 90] and references therein.

In general, non-Fickean behaviours can be gathered in two categories:

- (i) non-locality in time, which associates the mass flux of a given chemical agent with the concentration gradient of that agent through an integro-differential relationship, such as, for

68 example, those involving fractional time derivatives or fractional time integrals [9];

- 69 (ii) non-locality in space, which means that the mass flux vector of a species *cannot* be expressed  
70 as a point-wise linear function of the concentration gradient, as Fick’s law would prescribe.

71 In this work, we focus on the second type of non-locality, and we are interested in quantifying  
72 the spatial influence of the mass flux at a given point on “distant” points of a body. However, it  
73 is important to recall that non-locality is a broad notion [43, 47], which covers a wide spectrum  
74 of phenomena, from transport processes [44] to plasticity [2, 57] or visco-elasticity [10, 37], and  
75 depends on the intrinsic structure of the system to which it is referred and/or on its response to  
76 long-range stimuli. Moreover, non-locality can be introduced in different ways, e.g., by having  
77 recourse to higher-order gradient theories, as is the case for plasticity [2, 57, 109], or by assigning  
78 constitutive laws that feature integro-differential operators [72, 43]. In particular, the employment  
79 of integrals and derivatives of fractional order [92, 9, 12] has demonstrated to be an effective method  
80 in the description of various non-local phenomena [11, 18, 22], including non-Fickian diffusion  
81 [26, 82, 35, 86]. As pointed out in [35], the introduction of Fractional Calculus allows for the  
82 description of non-Fickian transport processes in a natural way, because of their close connection  
83 with the concept of anomalous diffusion [84].

84 Before going further, we notice that in the literature there exist other non-Fickian diffusion  
85 laws that, however, do not rely on the assumption of non-local effects. In particular, the Maxwell-  
86 Stefan model [71], which generalises Fick’s diffusion by the consideration of “*thermodynamic non-*  
87 *idealities*”<sup>1</sup> and “*influence of external force fields*”, has been postulated in the study of porous  
88 media and tumour growth [68].

## 89 1.1 Aim and novelties of our work

90 In the present work, on the basis of the indications given above, our aim is to highlight and  
91 study the influence of the non-local character of diffusion processes that could be acting in an  
92 avascular tumour. To accomplish this task, we propose a potentially new constitutive relationship  
93 of fractional type for the mass flux vector. Consequently, we refer only to fractional operators in  
94 space, so that the model is non-local in space but local in time. In our formulation, the mass flux  
95 vector of the chemical species, evaluated at a given spatial point, is put in relation, through an  
96 integral operator, to the concentration gradient of that species, evaluated at all other points of  
97 the region of space occupied by the tumour. This leads to a generalisation of Fick’s law that can  
98 be related to Fractional Calculus in a straightforward manner. In particular, this connection will  
99 become evident in the specification of the mass flux vector for the study of a benchmark problem  
100 (see Section “Definition of the non-locality function”).

101 For our purposes, we adopt part of the modelling assumptions outlined in [80, 101, 56, 91].  
102 Specifically, we study the tumour as a mixture comprising a fluid phase and a solid phase, and we  
103 identify its growth with the gain or loss of mass of the solid phase at the expenses or advantage of  
104 the fluid one. In particular, the model we employ predicts the gain of mass for a sufficiently high

---

<sup>1</sup>According to [115], the thermodynamic non-idealities are related to a phenomenon that pertains to a thermodynamic system, like, for instance, a gas, and that occurs through the “*storage of potential energy*” among the molecules of the system itself as a result of the interactions among such molecules. The main consequence of the non-idealities is that the concentrations of the molecules turn out to be different from those expected in the absence of the energy storage among them.

105 concentration of chemical agents (in fact, nutrients) and the loss of mass when the concentration  
106 of these falls below a certain threshold [81, 80]. Moreover, in the case of mass uptake of the solid  
107 phase, the model accounts for mechanotransduction [81, 80, 50, 56], thereby allowing a modulation  
108 of growth by means of stress [81, 80], whereas both for positive and for negative growth, the onset of  
109 structural transformations and their related inelastic distortions are considered. In the remainder  
110 of this work, we address only the most pertinent considerations and equations, while we refer the  
111 Reader to [80, 101, 91] for further details.

112 Before going further, we find it convenient to highlight the main novelties of our work, which  
113 can be summarised as follows:

- 114 1. *Impact of non-local diffusion on tumour growth.* With respect to [80, 101, 56, 91], we study the  
115 diffusion of the chemical agents in a growing tumour by hypothesising a non-local constitutive  
116 law for the diffusive mass flux vector. This is done with the purpose of weighing how and to  
117 which extent the deviation of non-local diffusion from the Fickian one impacts on the main  
118 descriptors of the tumour's evolution.
- 119 2. *Evolving non-locality driven by the tumour's dynamics.* The model that we are proposing  
120 requires to solve a type of non-locality that changes with the dynamics of the tumour through  
121 its motion *and* growth. To the best of our knowledge, this is a generalisation of a setting  
122 adopted in several papers (see e.g. [35, 63, 105, 75]), where the non-locality is accounted for  
123 in advection-diffusion equations without considering the deformation or structural change of  
124 the media in which such equations are defined.
- 125 3. *Non-locality and non-linearity.* The core of our work is the equation governing the evolution  
126 of chemical agents. This is given by an advection-diffusion-reaction equation featuring a  
127 fractional diffusive mass flux vector and a non-linear reaction term. We solve this equation  
128 *together* with all the other balance laws, expressed by non-linear partial differential equations,  
129 that model the tumour and its growth. Therefore, we solve a system of equations in which  
130 non-linearity combines with non-locality. To us, this is a novelty because, to the best of our  
131 knowledge, papers on Fractional Calculus usually solve one equation in conjunction with a  
132 fractional constitutive law. Furthermore, the nature of the problem we are tackling makes it  
133 impossible to have recourse to solution techniques based on Fourier and Laplace transforms,  
134 which are standard for problems of Fractional Calculus that are linear and/or formulated in  
135 unbounded domains. In our case, however, this assumption would be physically unrealistic  
136 and we have, thus, to turn to numerical techniques, such as Finite Element (FE) methods.

137 We point out that the study of fractional diffusion in bounded domains is delicate because  
138 of the complexity of the numerics involving operators of fractional type. Nevertheless, in the  
139 literature there exist some works dealing with fractional diffusion equations on bounded domains.  
140 The majority of these works employ finite-difference Grünwald-Letnikov discretisation schemes  
141 (see e.g. [88, 76, 36, 83]), and there also exist studies in which FE methods have been used for  
142 solving equations of fractional type [99, 63, 49, 44]. However, to the best of our knowledge, there  
143 is still a lack of studies addressing in detail the numerical issues arising in the context of fractional  
144 differential equations within a non-linear mechanical framework.

145 We also mention that, in this work, we suggest a possible way of formulating non-local diffusion  
146 on manifolds by adapting the definition of convolution on manifolds given in [106]. Originally, we  
147 encountered the necessity of expressing convolution in the non-Euclidean context because we aimed

148 at writing our model in fully covariant formalism as a first step towards non-Euclidean settings.  
 149 However, we faced some technical difficulties, which made us opt, for the time being, to give just a  
 150 sketch of the generalisation of non-local diffusion on manifolds. For this reason, we summarised the  
 151 main steps of our generalisation in Appendix A1. Note that Meerschaert et al. [82] did consider  
 152 diffusion-like problems on manifolds but within a different framework.

153 Finally, we would like to point out that, throughout this work, the terminologies “mass fraction”  
 154 and “concentration” will be often used interchangeably, and the spatial and temporal dependence  
 155 of the variables are dropped out, unless there is a necessity to account for the non-local character  
 156 of the problem, where this dependence is explicitly specified.

## 157 2 Kinematics

158 Let  $\mathcal{S}$  be the three-dimensional Euclidean space,  $\mathcal{T}$  an interval of time, and  $\mathcal{B} \subset \mathcal{S}$  the reference  
 159 placement of the mechanical system representing an avascular tumour, in which the tumour may,  
 160 or may not, be free of stress. In particular, we consider that the tumour is a saturated mixture  
 161 comprising a solid and a fluid phase. Moreover, the region of  $\mathcal{S}$  occupied by the system at time  
 162  $t \in \mathcal{T}$  is referred to as current configuration and is denoted by  $\mathcal{B}_t \equiv \chi(\mathcal{B}, t)$ , where  $\chi(\cdot, t) : \mathcal{B} \rightarrow \mathcal{S}$   
 163 describes the motion of the solid phase (for the mixture kinematics, we follow here the same  
 164 approach as the one adopted in [33]). Then, a point  $x \in \mathcal{B}_t$  is given by  $x = \chi(X, t)$ , with  
 165  $X \in \mathcal{B}$  and  $t \in \mathcal{T}$ . By differentiating the motion  $\chi$  with respect to  $X$ , we obtain the deformation  
 166 gradient tensor,  $\mathbf{F}$ , defined as the tangent map of  $\chi$ , i.e.,  $\mathbf{F}(\cdot, t) \equiv T\chi(\cdot, t) : T\mathcal{B} \rightarrow T\mathcal{S}$ ,  
 167 with  $T\mathcal{B} = \sqcup_{X \in \mathcal{B}} T_X \mathcal{B}$  and  $T\mathcal{S} = \sqcup_{x \in \mathcal{S}} T_x \mathcal{S}$ . Thus, tensor  $\mathbf{F}(X, t)$  characterises the visible  
 168 deformations of the system by mapping vectors of the tangent space  $T_X \mathcal{B}$  into the tangent space  
 169  $T_x \mathcal{S}$ .

170 We also introduce the spatial volumetric fractions of the solid and the fluid phases, given by  
 171  $\varphi_s(x, t)$  and  $\varphi_f(x, t)$ , respectively. Then, we define the *apparent* mass densities,  $\varphi_s(x, t)\varrho_s(x, t)$  and  
 172  $\varphi_f(x, t)\varrho_f(x, t)$ , of the solid and of the fluid, where  $\varrho_s(x, t)$  and  $\varrho_f(x, t)$  represent the *true* mass  
 173 densities of the solid and the fluid phase, respectively. We notice that the apparent mass densities  
 174 express, in each case, the phase mass per unit volume of the mixture as a whole, whereas each true  
 175 mass density is the inherent density of the corresponding phase. Furthermore, the saturation of  
 176 the mixture implies that  $\varphi_s(x, t) + \varphi_f(x, t) = 1$ , for all  $x \in \mathcal{B}_t$  and  $t \in \mathcal{T}$ .

177 The velocity of the mixture is  $\mathbf{v}(x, t) := \sum_{k \in \{s, f\}} \varphi_k(x, t)\varrho_k(x, t)\mathbf{v}_k(x, t)/\varrho(x, t)$ , where  $\mathbf{v}_s(x, t)$   
 178 and  $\mathbf{v}_f(x, t)$  denote the velocities of the solid and the fluid phases, respectively, and  $\varrho(x, t) :=$   
 179  $\sum_{k \in \{s, f\}} \varphi_k(x, t)\varrho_k(x, t)$  is the mass density of the mixture as a whole. We notice that, by intro-  
 180 ducing the solid phase velocity  $\mathbf{V}_s(X, t) := \dot{\chi}(X, t)$ , where the “dot” symbol denotes differentiation  
 181 with respect to time, the relationship  $\mathbf{v}_s(x, t) = \mathbf{v}_s(\chi(X, t), t) = \mathbf{V}_s(X, t)$  holds true for all  $X \in \mathcal{B}$   
 182 and  $t \in \mathcal{T}$ . Furthermore, since the tumour under study is assumed to be a mixture also in  $\mathcal{B}$ ,  
 183 the solid and the fluid coexist at every point  $X \in \mathcal{B}$ . This situation implies that any point  $x$  in  
 184 the fluid phase can be also viewed as the image of  $X$  through the motion  $\chi$  and, consequently,  
 185  $\mathbf{v}_f(x, t) = \mathbf{v}_f(\chi(X, t), t) = \mathbf{V}_f(X, t)$ .

## 186 2.1 Kinematics of growth

187 As suggested in several works, see e.g. [46, 110] and references therein, a relevant aspect in the  
 188 growth of a tumour is the manifestation of irreversible changes of its internal structure. To take  
 189 this aspect into account, we employ some concepts taken from the theory of inelastic processes.  
 190 Specifically, for characterising the growth of the tissue under study, we invoke the Bilby-Kröner-Lee  
 191 (BKL) decomposition of the deformation gradient tensor [85, 27, 102, 98, 52], i.e.,

$$\mathbf{F} = \mathbf{F}_e \mathbf{F}_\gamma, \quad (1)$$

192 where the generally non-integrable tensor fields  $\mathbf{F}_e$  and  $\mathbf{F}_\gamma$  describe the elastic accommodation of  
 193 the tumour and the inelastic distortions induced by growth, respectively. We denote by  $\mathcal{N}_t(X)$   
 194 the *natural state* of the body element of the tumour's solid phase associated with  $X$ , and we let  
 195 it represent a stress-free state. We refer to the tensor  $\mathbf{F}_\gamma(X, t): T_X \mathcal{B} \rightarrow \mathcal{N}_t(X)$  as *growth tensor*  
 196 and we assume that it comprehends the structural transformations undergone by the tumour in the  
 197 course of its evolution. Then, the accommodating elastic tensor  $\mathbf{F}_e(X, t)$  maps vectors of  $\mathcal{N}_t(X)$   
 198 into vectors of  $T_x \mathcal{S}$ . We refer to the works [102, 52, 94, 27, 101, 56], and references therein, for a  
 199 more complete discussion on the nature and generalisation of the multiplicative decomposition in  
 200 Equation (1).

201 In particular, following [80, 101, 56], in the present work we contemplate the case in which the  
 202 growth tensor is a pure dilatation, that is, we impose  $\mathbf{F}_\gamma = \gamma \mathbf{I}$ , where  $\gamma > 0$  is referred to as *growth*  
 203 *parameter* and  $\mathbf{I}$  is the second-order identity tensor.

## 204 3 Balance laws

205 By adopting the modelling assumptions made in [80, 101, 56], we consider that the fluid phase is  
 206 constituted by chemical agents and “water”, with mass fractions  $c_a$  and  $c_w$ , respectively, and such  
 207 that  $c_a + c_w = 1$ . Furthermore, we hypothesise the solid phase to consist of two type of cells, i.e.,  
 208 the proliferating cells, with mass fraction  $c_p$ , and the necrotic cells, with mass fraction  $c_n$ , where  
 209  $c_p + c_n = 1$ .

### 210 3.1 Mass balance laws

211 The mass balance laws for the gain and loss of mass of the proliferating and the necrotic cells, and  
 212 for the mass fraction of the chemical species and the fluid phase as a whole are

$$\partial_t(\varphi_s \varrho_s c_p) + \operatorname{div}(\varphi_s \varrho_s c_p \mathbf{v}_s) = r_{\text{pn}} + r_{\text{fp}}, \quad (2a)$$

$$\partial_t(\varphi_s \varrho_s c_n) + \operatorname{div}(\varphi_s \varrho_s c_n \mathbf{v}_s) = r_{\text{nf}} - r_{\text{pn}}, \quad (2b)$$

$$\partial_t(\varphi_f \varrho_f c_a) + \operatorname{div}(\varphi_f \varrho_f c_a \mathbf{v}_f + \mathbf{y}_\alpha) = r_{\text{ap}}, \quad (2c)$$

$$\partial_t(\varphi_f \varrho_f) + \operatorname{div}(\varphi_f \varrho_f \mathbf{v}_f) = -r_s, \quad (2d)$$

213 where  $r_{\text{pn}}$ ,  $r_{\text{fp}}$ ,  $r_{\text{nf}}$  and  $r_{\text{ap}}$  denote rates of mass intake and/or reduction [80, 101, 56]. Specifically,  
 214 they represent the rate at which the proliferating cells turn into necrotic ( $r_{\text{pn}}$ ), the mass from the  
 215 fluid phase that promotes the proliferation of cells ( $r_{\text{fp}}$ ), the necrotic cells that dissolve into the  
 216 fluid ( $r_{\text{nf}}$ ), and the chemical agents that are depleted by the proliferating cells ( $r_{\text{ap}}$ ). Moreover,



217  $r_s := r_{\text{fp}} + r_{\text{nf}}$  is the global source/sink of mass of the solid phase as a whole. Particularly, in  
 218 writing Equations (2a) and (2b), we have enforced the consideration that the two cell populations  
 219 move at the same velocity  $\mathbf{v}_s$ . In Equation (2c), the term  $\mathbf{y}_\alpha$  corresponds to the mass flux vector  
 220 of the chemical agents, and since the focus of this work is subordinate to its definition, we prefer  
 221 to make a deeper analysis of its characterisation and physical meaning in a separate section.

222 By enforcing that the tissue's cells are mainly composed by water [19, 80, 51], the true mass  
 223 density of the solid phase,  $\varrho_s$ , can be regarded as constant and equal to the true mass density of the  
 224 fluid phase,  $\varrho_f$ , which is set to be equal to the density of water. Thus, by taking into account the  
 225 saturation constraint and the BKL decomposition in Equation (1), Equations (2a)–(2d), written  
 226 with respect to the reference configuration, become

$$\dot{\mathbf{c}}_p = [R_{\text{pn}} + R_{\text{fp}} - R_s \mathbf{c}_p][J_\gamma \Phi_{s\nu} \varrho_s]^{-1}, \quad (3a)$$

$$\frac{\dot{\gamma}}{\gamma} = [R_{\text{fp}} + R_{\text{nf}}][3\varrho_s \Phi_{s\nu} J_\gamma]^{-1}, \quad (3b)$$

$$\varrho_f [J - J_\gamma \Phi_{s\nu}] \dot{\mathbf{c}}_a + \varrho_f \mathbf{Q} \text{Grad} \mathbf{c}_a + \text{Div} \mathbf{Y}_\alpha = \mathbf{c}_a R_s + R_{\text{ap}}, \quad (3c)$$

$$\text{Div} \mathbf{Q} + \dot{J} = 0, \quad (3d)$$

227 where the material filtration velocity  $\mathbf{Q}$ , the material mass flux vector of the chemical agents  $\mathbf{Y}_\alpha$ , the  
 228 mass fractions  $\mathbf{c}_a$  and  $\mathbf{c}_p$ , and the material sources/sinks of mass featuring in Equations (3a)–(3d)  
 229 are given by

$$\mathbf{Q}(X, t) := J(X, t) \mathbf{q}(\chi(X, t), t) \mathbf{F}^{-\text{T}}(X, t), \quad (4a)$$

$$\mathbf{Y}_\alpha(X, t) := J(X, t) \mathbf{y}_\alpha(\chi(X, t), t) \mathbf{F}^{-\text{T}}(X, t), \quad (4b)$$

$$\mathbf{c}_k(X, t) := c_k(\chi(X, t), t), \quad k \in \{a, p\} \quad (4c)$$

$$R_\beta(X, t) := J(X, t) r_\beta(\chi(X, t), t), \quad \beta \in \{\text{pn}, \text{fp}, \text{nf}, \text{ap}, \text{s}\}, \quad (4d)$$

230 with  $\mathbf{q} = \varphi_f [\mathbf{v}_f - \mathbf{v}_s]$ . We note that, in writing Equations (3a)–(3d), the material volumetric  
 231 fractions  $\Phi_s(X, t) := J(X, t) \varphi_s(\chi(X, t), t)$  and  $\Phi_f(X, t) := J(X, t) \varphi_f(\chi(X, t), t)$  have been written  
 232 as  $\Phi_s = J_\gamma \Phi_{s\nu}$  and  $\Phi_f = J - J_\gamma \Phi_{s\nu}$ , where  $\Phi_{s\nu}(X, t) := J_e(X, t) \varphi_s(\chi(X, t), t)$  is the “pull-back” of  
 233 the solid phase volumetric fraction,  $\varphi_s$ , to the natural state [101, 56]. In particular, by imposing  
 234 that the temporal derivative of  $J_\gamma$  compensates for the mass source  $r_s$  [42, 5], it can be deduced  
 235 that the volumetric fraction  $\Phi_{s\nu}$  is independent of time. However,  $\Phi_{s\nu}$  may depend on material  
 236 points [56]. Furthermore, since it holds true that  $J_e = J/J_\gamma$ , the volumetric fractions of the solid  
 237 and the fluid phase can be expressed entirely in terms of the volume ratios  $J$  and  $J_\gamma$ , i.e.,

$$\varphi_s(x, t) = \varphi_s(\chi(X, t), t) = \frac{J_\gamma(X, t) \Phi_{s\nu}(X)}{J(X, t)}, \quad (5a)$$

$$\varphi_f(x, t) = 1 - \varphi_s(x, t) = \frac{J(X, t) - J_\gamma(X, t) \Phi_{s\nu}(X)}{J(X, t)}. \quad (5b)$$

## 238 3.2 Momentum balance laws

239 In this work, we neglect inertial and body forces, so that the momentum balance laws for the  
 240 biphasic medium as a whole and for the fluid phase write [60, 54, 91]

$$\text{div}(\boldsymbol{\sigma}_s + \boldsymbol{\sigma}_f) = \mathbf{0}, \quad (6a)$$



$$\mathbf{q} = -\mathbf{k} \operatorname{grad} p, \quad (6b)$$

241 where  $\boldsymbol{\sigma}_s$  and  $\boldsymbol{\sigma}_f$  are the Cauchy stress tensors of the solid and the fluid phase,  $p$  is the hydrostatic  
 242 pressure, Equation (6b) expresses Darcy's law [60], and  $\mathbf{k}$  denotes the *permeability tensor*, which is  
 243 here taken to be symmetric and positive definite.

244 Following [60, 15, 53, 101], we assume the fluid phase to be macroscopically inviscid, so that  $\boldsymbol{\sigma}_f$   
 245 is purely hydrostatic, and we write

$$\boldsymbol{\sigma}_f = -\varphi_f p \mathbf{g}^{-1}, \quad (7a)$$

$$\boldsymbol{\sigma}_s = -\varphi_s p \mathbf{g}^{-1} + \boldsymbol{\sigma}_{sc}, \quad (7b)$$

246 where  $\boldsymbol{\sigma}_{sc}$  is said to be the constitutive part of  $\boldsymbol{\sigma}_s$  and  $\mathbf{g}^{-1}$  is the inverse of the metric tensor,  
 247  $\mathbf{g}$ , associated with  $\mathcal{S}$ . Then, by substituting Equations (7a) and (7b) into Equation (6a), and  
 248 performing the backward Piola transformation of Equations (6a) and (6b), we obtain

$$\operatorname{Div}(-J \mathbf{p} \mathbf{g}^{-1} \mathbf{F}^{-T} + \mathbf{P}_{sc}) = \mathbf{0}, \quad (8a)$$

$$\mathbf{Q} = -\mathbf{K} \operatorname{Grad} p, \quad (8b)$$

249 where we have introduced the notation

$$\mathbf{p}(X, t) := p(\chi(X, t), t), \quad (9a)$$

$$\mathbf{K}(X, t) := J(X, t) \mathbf{F}^{-1}(\chi(X, t), t) \mathbf{k}(\chi(X, t), t) \mathbf{F}^{-T}(X, t), \quad (9b)$$

$$\mathbf{P}_{sc}(X, t) := J(X, t) \boldsymbol{\sigma}_{sc}(\chi(X, t), t) \mathbf{F}^{-T}(X, t), \quad (9c)$$

$$\mathbf{g}(X, t) := \mathbf{g}(\chi(X, t)), \quad (9d)$$

250 to denote, respectively, the pressure expressed as a function of time and of the points of  $\mathcal{B}$ , the  
 251 material permeability tensor, the constitutive part of the overall first Piola-Kirchhoff stress tensor,  
 252 and the metric tensor expressed as a function of time and of the points of  $\mathcal{B}$ . Moreover, Equation  
 253 (8b) represents Darcy's law of filtration, pulled-back to the reference configuration.

## 254 4 Constitutive laws I: Strain energy density and per- 255 meability

256 Following [80, 101, 56], we hypothesise that the solid phase of the tumour is isotropic and hyperelas-  
 257 tic, and introduce the strain energy densities  $\mathcal{W}$  and  $\mathcal{W}_\nu$ , which are written per unit volume of the  
 258 reference configuration and of the natural state, respectively. To account for the structural changes  
 259 induced by growth, the strain energy density  $\mathcal{W}$  is expressed as a constitutive function, namely  
 260  $\check{\mathcal{W}}$ , depending on  $\mathbf{F}$ ,  $\mathbf{F}_\gamma$  and on material points. Furthermore, we denote by  $\check{\mathcal{W}}_\nu$  the constitutive  
 261 representation of  $\mathcal{W}_\nu$ , which is supposed here to depend solely on the tensor  $\mathbf{F}_e$ . Therefore, the  
 262 following relationship holds [42, 30, 101]

$$\check{\mathcal{W}}(\mathbf{F}(X, t), \mathbf{F}_\gamma(X, t), X) = J_\gamma(X, t) \check{\mathcal{W}}_\nu(\mathbf{F}_e(X, t)). \quad (10)$$

263 Within a more general framework, the strain energy density  $\check{\mathcal{W}}_\nu$  maintains the explicit dependence  
 264 on  $X$ , and Equation (10) does not hold in its present form. This becomes evident when  $\check{\mathcal{W}}_\nu$  is

parameterised by point-dependent material coefficients or, by expressing  $\check{W}_\nu$  as  $\check{W}_\nu = \Phi_{s\nu} \varrho_s \check{\Psi}_s$ , where  $\check{\Psi}_s$  is the solid phase strain energy density per unit mass, when  $\Phi_{s\nu}$  depends on  $X$ . However, these circumstances are excluded from the setting of this work, as can be deduced by looking at Table 1, in which all the material parameters and  $\Phi_{s\nu}$  are taken as constants.

Hereafter, we adopt a constitutive law of the type proposed in [62] for  $\check{W}_\nu$ , i.e.,

$$\check{W}_\nu(\mathbf{F}_e) = \hat{\mathcal{W}}_\nu(\mathbf{C}_e) = a_0 \{ \exp(\hat{\Psi}(\mathbf{C}_e)) - 1 \}, \quad (11a)$$

$$\hat{\Psi}(\mathbf{C}_e) = a_1 [\hat{I}_1(\mathbf{C}_e) - 3] + a_2 [\hat{I}_2(\mathbf{C}_e) - 3] - a_3 \log(\hat{I}_3(\mathbf{C}_e)), \quad (11b)$$

where  $\hat{\mathcal{W}}_\nu$  is the constitutive representation of  $\mathcal{W}$  expressed as a function of the elastic, right Cauchy-Green deformation tensor  $\mathbf{C}_e = \mathbf{F}_e^T \cdot \mathbf{F}_e = \mathbf{F}_\gamma^{-T} \mathbf{C} \mathbf{F}_\gamma^{-1}$ ,  $\mathbf{C} = \mathbf{F}^T \cdot \mathbf{F}$  is the ‘‘classical’’, right Cauchy-Green deformation tensor,  $\hat{I}_1(\mathbf{C}_e) = \text{tr}(\mathbf{C}_e)$ ,  $\hat{I}_2(\mathbf{C}_e) = \frac{1}{2} \{ [\hat{I}_1(\mathbf{C}_e)]^2 - \text{tr}[(\mathbf{C}_e)^2] \}$ , and  $\hat{I}_3(\mathbf{C}_e) = \det(\mathbf{C}_e)$  are the principal invariants of  $\mathbf{C}_e$ , and, as in [62, 114, 101], the parameters  $a_0$ ,  $a_1$ ,  $a_2$  and  $a_3$  are expressed in terms of Lamé’s parameters  $\lambda$  and  $\mu$ , i.e.,

$$a_0 = \frac{2\mu + \lambda}{4a_3}, \quad a_1 = a_3 \frac{2\mu - \lambda}{2\mu + \lambda}, \quad a_2 = a_3 \frac{\lambda}{2\mu + \lambda}, \quad a_3 = a_1 + 2a_2 = 1. \quad (12)$$

Then, by using Equations (11a) and (11b), the constitutive part of the first Piola-Kirchhoff stress tensor reads [101]

$$\mathbf{P}_{sc} = J_\gamma \mathbf{F} \mathbf{F}_\gamma^{-1} \left( 2 \frac{\partial \hat{\mathcal{W}}_\nu}{\partial \mathbf{C}_e}(\mathbf{C}_e) \right) \mathbf{F}_\gamma^{-T}. \quad (13)$$

Furthermore, we require the permeability tensor to be ‘‘unconditionally isotropic’’ [13], i.e.,  $\mathbf{k} = k_0 \mathbf{g}^{-1}$ , so that the material permeability tensor reads

$$\mathbf{K} = J k_0 \mathbf{C}^{-1}. \quad (14)$$

In Equation (14),  $k_0$  denotes the *scalar permeability* and is taken here as in [13, 62], i.e.,

$$k_0 = k_R \left[ \frac{J - J_\gamma \Phi_{s\nu}}{J_\gamma \varphi_{fR}} \right]^{m_0} \exp \left( \frac{m_1}{2} \left[ \frac{J^2 - J_\gamma^2}{J_\gamma^2} \right] \right), \quad (15)$$

where  $m_0$  and  $m_1$  are constant material coefficients,  $\varphi_{fR} := 1 - \Phi_{s\nu}$  is a reference value of the fluid phase volumetric fraction, and  $k_R$  is the reference permeability of the medium. In the sequel, both  $k_R$  and  $\varphi_{fR}$ , and thus  $\Phi_{s\nu}$ , are assumed to be constant.

## 5 Constitutive Laws II: Non-Fickian diffusion

As pointed out in the Introduction, our aim is to generalise previous models of tumour growth [80, 101] by using some of the notions and tools offered by the theory of Fractional Calculus [92, 9, 12]. To this end, we introduce a non-Fickian type of diffusion of the chemical agents. Specifically, our purpose is to take into account the non-local behaviour of the gradient of the chemical agents’ mass fraction, and study its influence on the growth of an avascular tumour.

## 289 5.1 Non-Fickian mass flux vector

290 We propose to express the chemical species' mass flux vector,  $\mathbf{y}_\alpha$  (see Equation (2c)), in terms  
 291 of a non-local constitutive law of convolution type, in which, in the Euclidean case, the kernel  
 292 of the convolution integral features a power law in the distance between the points  $x$  and  $\tilde{x}$   
 293 each pair  $(x, \tilde{x})$  of spatial points occupied by body points. This way, we aim to show how  $\mathbf{y}_\alpha$ ,  
 294 evaluated at  $x$ , depends on the gradients of concentration evaluated at all other points  $\tilde{x}$ , and on  
 295 the power law chosen for the convolution kernel. To do this, we face two difficulties: the first one  
 296 is connected to the fact that, since, for the sake of generality, we view the body as a manifold, the  
 297 concept of convolution has to be suitably generalised; the second one is due to the impossibility of  
 298 integrating vector fields on manifolds. Whereas the first issue has been investigated in the literature  
 299 [17, 106, 93], and we refer to the convolution on manifolds put forward in [106], the second issue  
 300 can be circumvented by re-defining the mass flux vector of the chemical agents in weak form, i.e.,  
 301 for each  $t \in \mathcal{T}$ , we define  $\mathbf{y}_\alpha$  through the *duality* product [16]

$$\langle \mathbf{y}_\alpha, \text{grad } \check{c} \rangle := -\varrho_f \int_{\mathcal{B}_t} \left\{ \int_{\mathcal{B}_t} [\text{grad } \check{c}(x)] \mathbf{d}_\alpha(x, \tilde{x}, t) [\text{grad } c_\alpha(\tilde{x}, t)] dv(\tilde{x}) \right\} dv(x), \quad (16a)$$

$$\mathbf{d}_\alpha(x, \tilde{x}, t) := \mathfrak{f}_\alpha(x, \tilde{x}) \mathfrak{d}_\alpha(x, \tilde{x}, t), \quad (16b)$$

302 for all  $\check{c} \in \check{\mathcal{C}} = \{\check{c} \in H^1(\mathcal{B}_t) : \check{c} = 0 \text{ on } (\partial\mathcal{B}_t)_D\}$ , with  $\check{\mathcal{C}}$  being the space of all *virtual variations*  
 303 *of the mass fractions*,  $(\partial\mathcal{B}_t)_D$  the portion of the boundary of  $\mathcal{B}_t$  on which Dirichlet conditions are  
 304 applied for the mass fraction of the chemical agents, and  $H^1(\mathcal{B}_t)$  is the standard Sobolev space of  
 305 square-integrable functions over  $\mathcal{B}_t$  whose weak derivatives up to the order one are square-integrable  
 306 over  $\mathcal{B}_t$  too.

307 We refer to the second-order tensor  $\mathbf{d}_\alpha(x, \tilde{x}, t)$  as *non-local diffusivity tensor*, and we express  
 308 it as the product of the scalar quantity  $\mathfrak{f}_\alpha(x, \tilde{x})$  and of the tensor  $\mathfrak{d}_\alpha(x, \tilde{x}, t)$ . In particular, for a  
 309 given  $x \in \mathcal{B}_t$  and varying  $\tilde{x} \in \mathcal{B}_t$ ,  $\mathfrak{f}_\alpha(x, \tilde{x})$ , referred to as the *non-locality function*, measures how  
 310 the intensity of the chemical signal expressed by  $\text{grad } c_\alpha(\tilde{x}, t)$  is felt at  $x$ . The tensor  $\mathfrak{d}_\alpha(x, \tilde{x}, t)$ ,  
 311 instead, is denominated *fractional diffusivity tensor*. We emphasise that  $\mathfrak{f}_\alpha$  is defined for  $x \neq \tilde{x}$   
 312 and that, since we are dealing with fractional diffusion, both  $\mathfrak{d}_\alpha(x, \tilde{x}, t)$  and  $\mathbf{d}_\alpha(x, \tilde{x}, t)$  have, in  
 313 general, physical dimensions different from those of the standard diffusivity tensor, depending on  
 314 the prescription of  $\mathfrak{f}_\alpha$  and  $\alpha \in \mathbb{R}^+$ .

315 The way in which  $\mathfrak{f}_\alpha(x, \tilde{x})$  is to be understood in the case in which  $\mathcal{B}_t$  is viewed as a manifold  
 316 is reported in Appendix A1. However, from here on, to avoid the technical difficulties of addressing  
 317 such a general framework, which is out of the scope of this work, we prefer to adopt orthogonal  
 318 Cartesian coordinates. Then, by regarding  $\mathcal{B}_t$  as a flat subset of  $\mathcal{S}$  having the same dimensionality  
 319 as  $\mathcal{S}$ ,  $\mathfrak{f}_\alpha(x, \tilde{x})$  can be recast in the form  $\mathfrak{f}_\alpha(x, \tilde{x}) = \hat{\mathfrak{f}}_\alpha(x - \tilde{x})$ , where  $\hat{\mathfrak{f}}_\alpha$  is introduced to re-define  $\mathfrak{f}_\alpha$  as  
 320 a function of the vector  $x - \tilde{x}$ , i.e., as  $\hat{\mathfrak{f}}_\alpha : T_{\tilde{x}}\mathcal{S} \rightarrow \mathbb{R}$  (see Appendix A1). Furthermore, we require  
 321  $\mathfrak{d}_\alpha(x, \tilde{x}, t)$  to be a two-point tensor of the type  $\mathfrak{d}_\alpha(x, \tilde{x}, t) = \sum_{a,b=1}^3 [\mathfrak{d}_\alpha(x, \tilde{x}, t)]^{ab} \mathbf{e}_a(x) \otimes \mathbf{e}_b(\tilde{x})$ ,  
 322 where  $\{\mathbf{e}_l(x)\}_{l=1}^3$  and  $\{\mathbf{e}_l(\tilde{x})\}_{l=1}^3$  are the vector bases attached to  $x$  and  $\tilde{x}$ . It is worth noticing  
 323 that, within a Cartesian setting, and for  $x = \tilde{x}$ , the tensor  $\mathbf{e}_a(x) \otimes \mathbf{e}_b(\tilde{x}) \equiv \mathbf{e}_a(x) \otimes \mathbf{e}_b(x)$  is referred  
 324 to as "*Jacoby directional tensor*" in [3], where, in a slightly different context, the central Marchaud  
 325 fractional derivative is extended to the case of two- or three-dimensional problems.

326 In general, there is no correlation at all between the vector bases  $\{\mathbf{e}_l(x)\}_{l=1}^3$  and  $\{\mathbf{e}_l(\tilde{x})\}_{l=1}^3$   
 327 and, in fact, each basis can be chosen arbitrarily and independently of the other one. Nevertheless,  
 328  $\{\mathbf{e}_l(\tilde{x})\}_{l=1}^3$  can be enforced to be the result of the parallel transport of  $\{\mathbf{e}_l(x)\}_{l=1}^3$  along the geodesic

329 connecting  $x$  and  $\tilde{x}$ . In particular, in the Euclidean case, the arch of the geodesic connecting  $x$  and  
330  $\tilde{x}$  is the segment of the straight line directed from  $x$  to  $\tilde{x}$  and the parallel transport of  $\{\mathbf{e}_l(x)\}_{l=1}^3$   
331 along such a line renders  $\{\mathbf{e}_l(\tilde{x})\}_{l=1}^3$  collinear with  $\{\mathbf{e}_l(x)\}_{l=1}^3$ . Hence, for each  $l = 1, 2, 3$ ,  $\mathbf{e}_l(x)$   
332 and  $\mathbf{e}_l(\tilde{x})$  can be associated with the same direction, hereafter denoted by  $\mathbf{i}_l$ , even though they  
333 remain, implicitly, distinct vectors, attached to different spatial points. Within this approach, we  
334 hypothesise that  $\mathfrak{d}_\alpha(x, \tilde{x}, t)$  admits the representation  $\mathfrak{d}_\alpha(x, \tilde{x}, t) = \sum_{b=1}^3 \mathfrak{d}_\alpha^b(x, \tilde{x}, t) \mathbf{e}_b(x) \otimes \mathbf{e}_b(\tilde{x})$   
335 and, since  $\mathbf{e}_l(x)$  is collinear with  $\mathbf{e}_l(\tilde{x})$ , this representation of  $\mathfrak{d}_\alpha(x, \tilde{x}, t)$  mimics the description of  
336 an orthotropic tensor function with respect to the set of directions  $\{\mathbf{i}_1, \mathbf{i}_2, \mathbf{i}_3\}$ . Hence, it is “as if”  
337 we had  $\mathfrak{d}_\alpha(x, \tilde{x}, t) = \sum_{b=1}^3 \mathfrak{d}_\alpha^b(x, \tilde{x}, t) \mathbf{i}_b \otimes \mathbf{i}_b$ . Then, by using the definitions in Equation (16), we  
338 identify the components of the fractional mass flux to be given by the following expression

$$[\mathbf{y}_\alpha(x, t)]^b := -\rho_f \int_{\mathcal{B}_t} \hat{\mathbf{f}}_\alpha(x - \tilde{x}) \mathfrak{d}_\alpha^b(x, \tilde{x}, t) \partial_b c_\alpha(\tilde{x}, t) \, \mathrm{d}\mathbf{v}(\tilde{x}), \quad \text{no sum over } b = 1, 2, 3, \quad (17)$$

339 and we call the coefficients  $\{\mathfrak{d}_\alpha^b(x, \tilde{x}, t)\}_{b=1}^3$  *fractional diffusivities*.

## 340 5.2 Comparison with other works

341 Other definitions of fractional mass flux vector can be found that characterise non-Fickian diffusion  
342 processes (see e.g. [82, 105] and references therein). For instance, Sapora et al. [105] study a  
343 fractional version of Darcy’s law in one dimension in which the filtration velocity (also known as  
344 “specific mass flux”) is taken to be proportional to an integral operator that the Authors refer  
345 to as “Riesz integral” [105] of pressure (note that the definition of Riesz integral given in [105]  
346 differs by a factor  $\cos(\beta\pi/2)$ , with  $\beta \in ]0, 1[$ , from that in [104, 9]). However, when passing to  
347 higher dimensionalities, it is necessary to extend the concept of fractional differentiation to other  
348 differential operators like the gradient of a scalar function. In this regard, in [40, 11, 113] the  
349 fractional gradient of order  $\alpha \in \mathbb{R}^+$  of a scalar function is defined as a co-vector, whose components  
350 are identified with the fractional partial derivatives, each of which of order  $\alpha$ , of the given function.  
351 In particular, these fractional partial derivatives are taken in the sense of Riemann-Liouville in [40]  
352 and in the sense of Caputo in [113], whereas the Nishimoto fractional derivative [87] is used in [1],  
353 for  $\alpha \in ]0, 1]$ .

354 For the purposes of our work, we adopt the definition given in Equation (17). This definition  
355 presents some fundamental differences with respect to the definition supplied, for instance, in [105].  
356 These differences, however, are not only related to the fact that the physical phenomenon addressed  
357 in [105] is distinct from the one we are studying here. Rather, they are intrinsic in the definition  
358 of the operator expressing  $\mathbf{y}_\alpha$ , and can be summarised as follows:

- 359 • Equation (17) is conceived in a three-dimensional setting and, consequently, requires an  
360 integration over the whole configuration of the body,  $\mathcal{B}_t$ , whereas the definition of the mass  
361 flux given in [105] features an integration over a bounded interval.
- 362 • In our definition, each fractional diffusivity  $\mathfrak{d}_\alpha^b(x, \tilde{x}, t)$ ,  $b = 1, 2, 3$ , is part of the integrand of  
363 Equation (17), and cannot be factorised out of the corresponding integral.
- 364 • If, for a given  $b_0 \in \{1, 2, 3\}$ , the fractional diffusivity  $\mathfrak{d}_\alpha^{b_0}(x, \tilde{x}, t)$  could be factorised out of  
365 the integral in Equation (17) (e.g. by setting  $\mathfrak{d}_\alpha^{b_0}(x, \tilde{x}, t) \equiv \mathfrak{d}_{0\alpha}$ , with  $\mathfrak{d}_{0\alpha}$  constant), and if

366 the only nonzero component of  $\text{grad } c(\tilde{x}, t)$  were  $\partial_{b_0} c_a(\tilde{x}, t)$  for all  $\tilde{x}$  and  $t$ , one would have

$$[\mathbf{y}_\alpha(x, t)]^{b_0} = -\varrho_f \mathfrak{D}_{0\alpha} \int_{\mathcal{B}_t} \hat{f}_\alpha(x - \tilde{x}) \partial_{b_0} c_a(\tilde{x}, t) \text{d}v(\tilde{x}), \quad (18)$$

367 where  $\hat{f}_\alpha(x - \tilde{x})$  is still a function of *all* the components of the vector  $x - \tilde{x}$ , rather than of  
 368 its  $b_0$ -th component only. This property marks a major difference between our approach and  
 369 the model developed in [105], and expresses the fact that, even in the presence of a preferred  
 370 direction (i.e., the one associated with  $\partial_{b_0} c_a$ ), one should account for the non-locality in all  
 371 directions.

372 Before going further, we notice that, if the fractional diffusivities  $\{\mathfrak{D}_\alpha^b(x, \tilde{x}, t)\}_{b=1}^3$  are all equal  
 373 to some reference constant value  $\mathfrak{D}_{R\alpha}$  (note that, for simplicity, we call ‘fractional diffusivities’ the  
 374 *set of the three principal fractional diffusivities*), the mass flux vector  $\mathbf{y}_\alpha(x, t)$  can be expressed (in  
 375 a Cartesian setting) as

$$\mathbf{y}_\alpha(x, t) = -\varrho_f \mathfrak{D}_{R\alpha} \int_{\mathcal{B}_t} \hat{f}_\alpha(x - \tilde{x}) \text{grad } c_a(\tilde{x}, t) \text{d}v(\tilde{x}). \quad (19)$$

376 Moreover, for some suitable  $\hat{f}_\alpha(x - \tilde{x})$ , usually written as a power-law that decays in space, the  
 377 integral on the right-hand-side of Equation (19) can be taken as the definition of a *fractional*  
 378 *gradient* of  $c_a$  of order  $\alpha$ , i.e., one can write (in the Cartesian setting)

$$\text{grad}^\alpha c_a(x, t) := \int_{\mathcal{B}_t} \hat{f}_\alpha(x - \tilde{x}) \text{grad } c_a(\tilde{x}, t) \text{d}v(\tilde{x}), \quad (20a)$$

$$[\text{grad}^\alpha c_a(x, t)]_b := \int_{\mathcal{B}_t} \hat{f}_\alpha(x - \tilde{x}) \partial_b c_a(\tilde{x}, t) \text{d}v(\tilde{x}), \quad b = 1, 2, 3. \quad (20b)$$

379 Equations (20a) and (20b) are reminiscent of the definition of fractional gradient of order  $\alpha$  supplied  
 380 in [113]. However, an important difference between that definition and ours is that, in [113], the  
 381 components of the fractional gradient of  $c_a$  (i.e.,  $\{[\text{grad}^\alpha c_a(x, t)]_b\}_{b=1}^3$  in our notation) are identified  
 382 with the Caputo derivatives of  $c_a$  along the principal directions of the vector basis. This, in turn,  
 383 requires the function  $\hat{f}_\alpha$  of Tarasov [113] to depend, for each Caputo derivative, solely on the  $b$ -th  
 384 component of  $x - \tilde{x}$ .

### 385 5.3 Backward Piola transform of the mass flux vector

386 The backward Piola transformation of Equation (16a) is given by

$$\begin{aligned} \langle \mathbf{y}_\alpha, \text{grad} \check{c} \rangle &= \langle \mathbf{Y}_\alpha, \text{Grad} \check{c} \rangle \\ &= -\varrho_f \int_{\mathcal{B}} \left\{ \int_{\mathcal{B}} [\text{Grad} \check{c}(X, t)] \mathbf{D}_\alpha(X, \tilde{X}, t) [\text{Grad } \mathbf{c}_a(\tilde{X}, t)] \text{d}V(\tilde{X}) \right\} \text{d}V(X), \end{aligned} \quad (21)$$

387 with  $\check{c}$  and  $\mathbf{c}_a$  such that  $\check{c}(X, t) = \check{c}(\chi(X, t))$  and  $\mathbf{c}_a(X, t) = c_a(\chi(X, t), t)$ , and we introduced the  
 388 *material non-local diffusivity tensor*,  $\mathbf{D}_\alpha$ , the *material non-locality function*,  $\mathfrak{F}_\alpha$ , and the *material*  
 389 *fractional diffusivity tensor*,  $\mathfrak{D}_\alpha$ , as follows

$$\mathbf{D}_\alpha(X, \tilde{X}, t) := J(X, t) \mathfrak{F}_\alpha(X, \tilde{X}, t) \mathfrak{D}_\alpha(X, \tilde{X}, t), \quad (22a)$$

$$\mathfrak{F}_\alpha(X, \tilde{X}, t) := \hat{f}_\alpha(\chi(X, t) - \chi(\tilde{X}, t)), \quad (22b)$$

$$\mathfrak{D}_\alpha(X, \tilde{X}, t) := J(\tilde{X}, t) \mathbf{F}^{-1}(\chi(X, t), t) \mathfrak{d}_\alpha(\chi(X, t), \chi(\tilde{X}, t), t) \mathbf{F}^{-T}(\tilde{X}, t). \quad (22c)$$

390 More specifically, the components of  $\mathfrak{D}_\alpha(X, \tilde{X}, t)$  and  $\mathbf{Y}_\alpha(X, t)$  are given by

$$[\mathfrak{D}_\alpha(X, \tilde{X}, t)]^{AB} = J(\tilde{X}, t) \sum_{b=1}^3 [\mathbf{F}^{-1}(\chi(X, t), t)]^A_b \mathfrak{d}_\alpha^b(\chi(X, t), \chi(\tilde{X}, t), t) [\mathbf{F}^{-T}(\tilde{X}, t)]_b^B, \quad (23a)$$

$$[\mathbf{Y}_\alpha(X, t)]^A = -\varrho_f \int_{\mathcal{B}} J(X, t) \mathfrak{F}_\alpha(X, \tilde{X}, t) \sum_{B=1}^3 [\mathfrak{D}_\alpha(X, \tilde{X}, t)]^{AB} \partial_B \mathbf{c}_a(\tilde{X}, t) dV(\tilde{X}). \quad (23b)$$

391 Expression (23b) defines the components of the mass flux vector in the material description, whereas  
 392  $\mathfrak{D}_\alpha$  is the material counterpart of the fractional diffusivity tensor  $\mathfrak{d}_\alpha$ .

393 In the sequel, we assume the spatial fractional diffusivities to be all equal to each other, i.e.,  
 394  $\mathfrak{d}_\alpha^b(x, \tilde{x}, t) = \mathfrak{d}_\alpha(x, \tilde{x}, t)$ , for all  $b = 1, 2, 3$ , and that  $\mathfrak{d}_\alpha(x, \tilde{x}, t)$  is independent of  $x$  (more rigorously,  
 395 we should say that  $\mathfrak{d}_\alpha$  can be redefined as a function of time and of the spatial variable with respect  
 396 to which the integration is made, i.e.,  $\tilde{x}$ ). Consequently, with a slight abuse of notation, we simply  
 397 write  $\mathfrak{d}_\alpha(\tilde{x}, t)$ . Moreover, following [101], we impose that  $\mathfrak{d}_\alpha(\tilde{x}, t)$  depends on position and time  
 398 through the volumetric fraction of the fluid phase, thereby setting  $\mathfrak{d}_\alpha(\tilde{x}, t) = \varphi_f(\tilde{x}, t) \mathfrak{d}_{R\alpha}$ , where  
 399  $\mathfrak{d}_{R\alpha}$  is a *reference fractional diffusivity*, which is parameterised by  $\alpha$ . Since  $\varphi_f(\tilde{x}, t)$  can be related  
 400 to the volumetric deformation of the solid phase and to growth through the expression (5b), we  
 401 obtain

$$\mathfrak{d}_\alpha(\chi(\tilde{X}, t), t) = \frac{J(\tilde{X}, t) - J_\gamma(\tilde{X}, t) \Phi_{sv}}{J(\tilde{X}, t)} \mathfrak{d}_{R\alpha}. \quad (24)$$

402 These considerations imply that the components of  $\mathfrak{D}_\alpha$  can be written as follows

$$[\mathfrak{D}_\alpha(X, \tilde{X}, t)]^{AB} = (J(\tilde{X}, t) - J_\gamma(\tilde{X}, t) \Phi_{sv}) \mathfrak{d}_{R\alpha} [\mathbf{F}^{-1}(\chi(X, t), t)]^A_b [\mathbf{F}^{-T}(\tilde{X}, t)]_b^B. \quad (25)$$

403 We notice that the non-local nature of the problem is also reflected in Equation (25). Indeed, in  
 404 a model accounting only for local interactions, the last two terms of Equation (25) would give the  
 405 inverse of the right Cauchy-Green deformation tensor  $\mathbf{C}$ , i.e.,  $\mathbf{C}^{-1} = \mathbf{F}^{-1} \mathbf{F}^{-T}$ , since  $X$  and  $\tilde{X}$   
 406 would coincide. Still, this is not true in our case, since the non-locality changes with the dynamics  
 407 of the tissue. Moreover, even in the case in which all the fractional diffusivities  $\{\mathfrak{d}_\alpha^b(x, \tilde{x}, t)\}_{b=1}^3$   
 408 were independent of  $x$  and  $\tilde{x}$ , their material counterparts  $\{[\mathfrak{D}_\alpha(X, \tilde{X}, t)]^{AB}\}_{A,B=1}^3$  would still be  
 409 functions of the points  $X$  and  $\tilde{X}$  because of the motion,  $\chi$ .

410 **Remark 1** *Due to the non-local nature of the mass flux vector, its Piola transformation needs to*  
 411 *be performed in two steps, i.e., as many as the integrals appearing in Equation (16a), or Equation*  
 412 *(21). In particular, the volume ratio  $J(X, t)$  is due to the change of measure of the outermost in-*  
 413 *tegral of Equation (21), which re-defines the duality product between  $\mathbf{y}_\alpha$  and  $\text{grad}\check{c}$  into the duality*  
 414 *product between  $\mathbf{Y}_\alpha$  and  $\text{Grad}\check{c}$ . In our formalism, this volume ratio is used to define the pull-back*  
 415 *of the non-local diffusivity tensor,  $\mathfrak{d}_\alpha$ , as prescribed by Equations (22a)–(22c). Furthermore, the*  
 416 *tensor  $\mathbf{F}^{-1}(\chi(X, t), t)$  featuring in Equation (22c) stems from the transformation of the gradient*  
 417 *of the virtual concentration,  $\check{c}$ , evaluated at  $x$ , i.e.,  $\text{grad}\check{c}(\chi(X, t), t) = \text{Grad}\check{c}(X, t) \mathbf{F}^{-1}(\chi(X, t), t)$ ,*

418 and it contributes, “from the left”, to the calculation of the pull-back of the fractional diffusivity  
419 tensor. Whereas this first part of the backward Piola transformation of the mass flux vector is  
420 standard, the second part of it reveals the non-locality of the constitutive law in Equation (21).  
421 Indeed, the tensor  $\mathbf{F}^{-\text{T}}(\tilde{X}, t)$  featuring in Equation (22c) must be evaluated in  $\tilde{X}$  because it origi-  
422 nates from the transformation of the gradient of the concentration (not the virtual one), which is  
423 part of the integrand of the innermost integral, i.e., the one expressing the non-local constitutive  
424 law. This tensor contributes, “from the right”, to determine the pull-back of the fractional diffu-  
425 sivity tensor. Finally, the volume ratio  $J(\tilde{X}, t)$  is necessary because of the change of measure in  
426 the innermost integral of Equation (16a) and is employed to define the pull-back of the fractional  
427 diffusivity tensor,  $\mathfrak{D}_\alpha$ . In conclusion, to determine the pull-back of the mass flux vector, a “double”  
428 Piola transformation has to be performed.

429 **Remark 2** Looking at the Piola transformation of the mass flux vector, it is worth mentioning  
430 that the non-locality of the problem, expressed through  $\hat{f}_\alpha$  as a function of  $(x - \tilde{x})$  in the current  
431 configuration, cannot be described in general as a function of  $(X - \tilde{X})$  in the reference configuration.  
432 Rather, the material non-locality function,  $\mathfrak{F}_\alpha$ , must be conceived as a function of the three variables  
433  $X$ ,  $\tilde{X}$  and  $t$  since, as prescribed by Equation (22b), it inherits this dependence from the motion,  $\chi$ ,  
434 in a way that, in general, cannot be reduced to a function of time and of the difference  $(X - \tilde{X})$ .  
435 Furthermore, we notice that the non-locality of the problem evolves from the reference to the current  
436 configuration. Indeed, two points that are “close” in  $\mathcal{B}$  can either be “far away” from each other  
437 or become “even closer” in  $\mathcal{B}_t$ , and vice versa.

## 438 6 Model summary and some numerical aspects

439 In this section, we summarise the equations characterising our mathematical model, specify the  
440 expressions for the sinks and sources of mass, and highlight some computational aspects to be  
441 taken into account. In the following, we focus on the case in which the considered chemical agents  
442 are nutrient substances that are necessary to trigger and maintain the growth of the tumour. Hence,  
443 we shall be referring to “nutrients” in lieu of “chemical agents” from here on.

### 444 6.1 Model equations

445 Our model is based on the following set of non-linear and coupled equations

$$\dot{\mathbf{c}}_{\text{p}} = [R_{\text{pn}} + R_{\text{fp}} - R_{\text{s}}\mathbf{c}_{\text{p}}][J_\gamma \Phi_{\text{s}\nu} \varrho_{\text{s}}]^{-1}, \quad (26\text{a})$$

$$\frac{\dot{\gamma}}{\gamma} = [R_{\text{fp}} + R_{\text{nf}}][3\varrho_{\text{s}}\Phi_{\text{s}\nu}J_\gamma]^{-1}, \quad (26\text{b})$$

$$\varrho_{\text{f}}[J - J_\gamma \Phi_{\text{s}\nu}]\dot{\mathbf{c}}_{\text{a}} - \varrho_{\text{f}}[\mathbf{K} \text{Grad} \mathbf{p}] \text{Grad} \mathbf{c}_{\text{a}} + \text{Div} \mathbf{Y}_\alpha = \mathbf{c}_{\text{a}} R_{\text{s}} + R_{\text{ap}}, \quad (26\text{c})$$

$$\dot{J} - \text{Div}(\mathbf{K} \text{Grad} \mathbf{p}) = 0, \quad (26\text{d})$$

$$\text{Div}(-J\mathbf{p}\mathbf{g}^{-1}\mathbf{F}^{-\text{T}} + \mathbf{P}_{\text{sc}}) = \mathbf{0}, \quad (26\text{e})$$



446 in the (4+3) unknowns  $\mathcal{U} := \{\mathbf{c}_p, \gamma, \mathbf{c}_a, \mathbf{p}, \{\chi^a\}_{a=1}^3\}$ , and with the source and sink terms [80, 101, 81]  
 447

$$R_{\text{fp}} = J\zeta_{\text{fp}} \left\langle \frac{\mathbf{c}_a - \mathbf{c}_{\text{cr}}}{\mathbf{c}_{\text{env}} - \mathbf{c}_{\text{cr}}} \right\rangle_+ \left[ 1 - \frac{\delta_1 \langle \bar{\sigma} \rangle_+}{\delta_2 + \langle \bar{\sigma} \rangle_+} \right] \underbrace{\frac{J - J_\gamma \Phi_{\text{sv}}}{J\varphi_{\text{fR}}}}_{=\varphi_{\text{f}}/\varphi_{\text{fR}}} \underbrace{\frac{J_\gamma \Phi_{\text{sv}}}{J}}_{=\varphi_{\text{s}}} \mathbf{c}_p, \quad (27a)$$

$$R_{\text{nf}} = -J\zeta_{\text{nf}} \frac{J_\gamma \Phi_{\text{sv}}}{J} (1 - \mathbf{c}_p), \quad (27b)$$

$$R_{\text{ap}} = -J\zeta_{\text{ap}} \frac{\mathbf{c}_a}{\mathbf{c}_a + \mathbf{c}_0} \frac{J_\gamma \Phi_{\text{sv}}}{J} \mathbf{c}_p, \quad (27c)$$

$$R_{\text{pn}} = -J\zeta_{\text{pn}} \left\langle 1 - \frac{\mathbf{c}_a}{\mathbf{c}_{\text{cr}}} \right\rangle_+ \frac{J_\gamma \Phi_{\text{sv}}}{J} \mathbf{c}_p. \quad (27d)$$

448 In Equations (27a)–(27c),  $\zeta_{\text{fp}}$ ,  $\zeta_{\text{nf}}$ ,  $\zeta_{\text{ap}}$  and  $\zeta_{\text{pn}}$  are constants indicating the characteristic time  
 449 scales with which the interstitial fluid is absorbed by the proliferating cells, the necrotic cells  
 450 go into the fluid, nutrients are consumed, and proliferating cells die, respectively. The operator  
 451  $\langle f \rangle_+ := \max\{0, f\}$  represents Macaulay’s brackets, which return the positive part of a function  $f$ .  
 452 Moreover,  $\mathbf{c}_{\text{cr}}$  is a critical value for the nutrients’ mass fraction and  $\mathbf{c}_{\text{env}}$  refers to the concentration  
 453 of nutrients present in the surrounding of the tumour. In order for growth to occur, it is necessary  
 454 that  $R_{\text{fp}} = Jr_{\text{fp}} > 0$ , i.e., it must hold that  $\mathbf{c}_a > \mathbf{c}_{\text{cr}}$ , provided  $\mathbf{c}_{\text{env}} > \mathbf{c}_{\text{cr}}$ . We also mention that the  
 455 mass source  $R_{\text{fp}}$  features the term in square brackets depending on  $\bar{\sigma} := -\frac{1}{3}\text{tr}\boldsymbol{\sigma}$ , which is introduced  
 456 in order to describe the fact that growth can be modulated by mechanical stress, thereby giving rise  
 457 to a phenomenon known as *mechanotransduction* [81, 80, 50, 56]. Finally, the product of the last  
 458 three factors in Equation (27a) describes the fact that, to allow for the transfer of mass from the  
 459 fluid to the proliferating cells, there must be a nonzero volumetric fraction of the fluid phase and  
 460 of the solid phase as well as a nonzero mass fraction of the proliferating cells. Macaulay’s brackets  
 461 in Equation (27d) ensure that the proliferating cells become necrotic, i.e.,  $R_{\text{pn}} < 0$  when  $\mathbf{c}_a < \mathbf{c}_{\text{cr}}$ ,  
 462 and  $R_{\text{pn}} = 0$  otherwise. Equation (27b) assumes that  $R_{\text{nf}}$  is linear in the volumetric fraction of  
 463 the solid phase and in the mass fraction of the necrotic cells, i.e.,  $1 - \mathbf{c}_p$ , while  $R_{\text{ap}}$  establishes that  
 464 the magnitude with which the nutrients are “eaten” by the proliferating cells depends on the ratio  
 465  $\mathbf{c}_a/\mathbf{c}_0$ , with  $\mathbf{c}_0 \in ]0, 1]$  being a reference value of the nutrients’ concentration that modulates their  
 466 consumption. We refer the Reader to [81, 80, 101, 56] for further details on these terms, and for  
 467 their generalisation to include growth-induced structural transformations.

468 Finally, we recall that the main goal of our model is to quantify the impact of the non-local  
 469 diffusion of the nutrients, accounted for by  $\mathbf{Y}_\alpha$ , on the overall evolution of the tumour, i.e., on all  
 470 the unknowns of the model. We note that, apart from the presence of the fractional mass flux  
 471 vector  $\mathbf{Y}_\alpha$ , our model is the same as the one presented in [80] and extended in [101, 56].

## 472 6.2 Numerical aspects

473 The model summarised in Equation (26) features ordinary differential equations, partial differential  
 474 equations and an integro-differential equation of fractional type. Since the model is formulated for  
 475 a bounded domain and many couplings and nonlinearities are accounted for, the usual techniques  
 476 adopted in Fractional Calculus for linear problems, such as the Fourier and Laplace transforms,  
 477 cannot be used. Consequently, we need to resort to numerical techniques. In particular, we solve

478 Equations (26a)–(26e) by means of a FE scheme that we need to adapt to our purposes in order  
 479 to take fractional derivatives into account. Here, we do not intend to go into the details of the  
 480 numerical scheme, which is out of the scope of this work. Nevertheless, we intend to give some  
 481 insights about the most important computational aspects of our work, while the numerical solutions  
 482 are obtained by using COMSOL Multiphysics®.

483 Classical FE techniques [55, 103] have been used for solving numerically Equations (26a), (26b),  
 484 (26d) and (26e), while Equation (26c) has required a special care. To this end, we report explicitly  
 485 only the weak formulation corresponding to it. Before doing this, we denote with  $(\partial\mathcal{B})_D$  and  $(\partial\mathcal{B})_N$   
 486 the Dirichlet and Neumann boundaries of  $\mathcal{B}$ , respectively, and assume  $\partial\mathcal{B} = (\partial\mathcal{B})_D \sqcup (\partial\mathcal{B})_N$ .  
 487 Furthermore, by using the standard formalism for Sobolev spaces [16], and using the space of  
 488 virtual concentrations,  $\check{C}_R := \{\check{c} \in H^1(\mathcal{B}) \text{ s.t. } \check{c}|_{(\partial\mathcal{B})_D} = 0\}$ , we have that, for all  $\check{c} \in \check{C}_R$ , the  
 489 following weak form applies

$$\begin{aligned} & \int_{\mathcal{B}} \{\varrho_f[J - J_\gamma \Phi_{sv}] \dot{c}_a - \varrho_f[\mathbf{K} \text{Grad} \mathbf{p}] \text{Grad} c_a - c_a R_s - R_{ap}\} \check{c} dV \\ & - \int_{\mathcal{B}} \mathbf{Y}_\alpha \text{Grad} \check{c} dV + \int_{(\partial\mathcal{B})_N} \mathbf{Y}_\alpha \cdot \mathbf{N} \check{c} dS = 0, \end{aligned} \quad (28)$$

490 where  $\mathbf{N}$  is the field of unit vectors normal to  $(\partial\mathcal{B})_N$  while  $\mathbf{Y}_\alpha$  is given in Equation (21), so that  
 491 the second volume integral of Equation (28) (without the sign) becomes

$$\begin{aligned} & \int_{\mathcal{B}} \mathbf{Y}_\alpha(X, t) \text{Grad} \check{c}(X, t) dV(X) \\ & = -\varrho_f \int_{\mathcal{B}} \left\{ \int_{\mathcal{B}} [\text{Grad} \check{c}(X, t)] \mathbf{D}_\alpha(X, \tilde{X}, t) [\text{Grad} c_a(\tilde{X}, t)] dV(\tilde{X}) \right\} dV(X). \end{aligned} \quad (29)$$

492 After applying a backward Euler scheme for the time derivative, a linearisation procedure, and  
 493 Galerkin method, Equation (28) leads to a system of algebraic equations that, except for a *non-local*  
 494 *stiffness matrix*, arising from the double integral in Equation (29), is similar to the one obtained in  
 495 standard FE approaches. From a numerical point of view, the non-local stiffness matrix reflects a  
 496 long range coupling among the elements in the spatial discretisation. Indeed, it is worth noting that,  
 497 in the construction of the non-local stiffness matrix, the cross integrations between the piecewise  
 498 polynomial *ansatz* functions do not vanish as they would in the case of the stiffness matrix of  
 499 a standard diffusion problem. That is, even though two discretisation nodes are far away from  
 500 each other, the entry of the matrix corresponding to these nodes will be non-zero, because of the  
 501 presence of the non-locality function  $\hat{f}_\alpha$ . This results into stiffness matrices that are denser, the  
 502 stronger the non-locality is. In fact, this is a typical feature of the numerical study of non-local  
 503 differential equations based on the use of FE methods (see for instance [47]). Still, as pointed out  
 504 in [47], standard techniques for the solution of such equations, like Gauss elimination, can be used.

505 Before closing this section, we would like to remark that, in the simulations carried out in our  
 506 work, the stiffness matrix associated with Equation (29) is symmetric and positive definite.

## 507 7 Benchmark problem and considerations on the non- 508 locality function

509 In this section, we specify a benchmark problem in order to simplify and solve the mathematical  
510 model given by Equations (26a)-(26e). To this end, we make use of the problem proposed in [5],  
511 and recently investigated in [101, 56] to account for growth-induced inelastic distortions. By doing  
512 this, we intend to model the volumetric growth of an avascular tumour in a “jacketed” cylindrical  
513 sample (its deformation is restricted to be along the longitudinal axis only), and to investigate, how  
514 and to what extent, the non-local diffusivity properties of the nutrients influence the dynamics of  
515 the tissue. In the following, we assume that the problem complies with axial symmetry and that  
516 it is radially homogeneous regardless of how slender the cylindrical sample is. This will require  
517 suitable *a priori* restrictions on all the unknowns of the problem.

### 518 7.1 Description of the benchmark problem

519 As in [101, 56], we adopt the cylindrical coordinates  $(R, \Theta, Z)$  and  $(r, \vartheta, z)$ , associated with the  
520 reference and the current configurations of the tumour, respectively. Moreover, we require the  
521 motion to satisfy with the conditions

$$\chi^r(R, \Theta, Z, t) = r = R, \quad (30a)$$

$$\chi^\vartheta(R, \Theta, Z, t) = \vartheta = \Theta, \quad (30b)$$

$$\chi^z(R, \Theta, Z, t) = z = Z + u(Z, t), \quad (30c)$$

522 where  $u$  is the unknown axial component of displacement. In this situation, the tumour is allowed  
523 to expand itself solely along the axial direction and  $\chi^z$  is the only unknown component of the  
524 motion,  $\chi$ . Additionally, to comply with the axial symmetry and with the radial homogeneity of  
525 the problem, the pressure  $\mathbf{p}$  is considered to be a function of the axial coordinate and time only.  
526 Another restriction pertains to the growth parameter  $\gamma$ , which is also assumed to depend only on  
527  $Z$  and  $t$  (note that since the growth tensor  $\mathbf{F}_\gamma = \gamma \mathbf{I}$  is spherical, it maintains the symmetries of  
528 the problem). Similar requirements also apply for the mass fraction of the proliferating cells,  $\mathbf{c}_p$ ,  
529 as well as for the mass fraction of the nutrients,  $\mathbf{c}_a$ .

530 The motion we have assumed implies that the matrix representations of the deformation gra-  
531 dient tensor  $\mathbf{F}$  and of the right Cauchy-Green deformation tensor  $\mathbf{C}$  read

$$[\mathbf{F}] = \text{diag}\{1, 1, 1 + u'\}, \quad (31a)$$

$$[\mathbf{C}] = \text{diag}\{1, 1, [1 + u']^2\}, \quad (31b)$$

532 where  $u'$  denotes the derivative of  $u$  in the axial direction. Since it holds that  $J = \det(\mathbf{F}) = 1 + u' >$   
533  $0$ ,  $u'$  must obey the inequality  $u' > -1$ .

534 Additionally, the growth tensor admits the diagonal form

$$[\mathbf{F}_\gamma] = \text{diag}\{\gamma, \gamma, \gamma\}, \quad \gamma > 0, \quad (32)$$

535 and, consequently, the elastic right Cauchy-Green deformation tensor  $\mathbf{C}_e$  has the representation

$$[\mathbf{C}_e] = \text{diag} \left\{ \frac{1}{\gamma^2}, \frac{1}{\gamma^2}, \frac{[1 + u']^2}{\gamma^2} \right\}. \quad (33)$$

536 Because of Equations (31a), (31b), (32) and (33), of the symmetry properties of the pressure  
 537 term  $-J\mathbf{p}\mathbf{g}^{-1}\mathbf{F}^{-\text{T}}$ , and of the constitutive expression (13), the first Piola-Kirchhoff stress tensor  
 538  $\mathbf{P} = -J\mathbf{p}\mathbf{g}^{-1}\mathbf{F}^{-\text{T}} + \mathbf{P}_{\text{sc}}$  has the diagonal representation

$$[\mathbf{P}] = \text{diag} \left\{ -J\mathbf{p} + [\mathbf{P}_{\text{sc}}]^{rR}, -J\mathbf{p} + [\mathbf{P}_{\text{sc}}]^{\vartheta\Theta}, -\mathbf{p} + [\mathbf{P}_{\text{sc}}]^{zZ} \right\}, \quad (34)$$

539 where each quantity featuring in each component of  $\mathbf{P}$  is a function solely of  $Z$  and time. Moreover,  
 540 it applies that  $[\mathbf{P}_{\text{sc}}]^{rR} = [\mathbf{P}_{\text{sc}}]^{\vartheta\Theta}$  and, thus, the balance of linear momentum (26e) in cylindrical  
 541 coordinates reduces to

$$\frac{\partial}{\partial Z} (-\mathbf{p} + [\mathbf{P}_{\text{sc}}]^{zZ}) = 0. \quad (35)$$

542 This result can be found also in other benchmark problems, such as the confined compression  
 543 tests of articular cartilage, under symmetry assumptions similar to those made here. Therefore,  
 544 Equation (35) constitutes a simplification obtained by virtue of symmetry and not by invoking the  
 545 slenderness of the cylinder used in our benchmark (see Table 1).

546 Note also that, according to Equations (14) and (15), the conditions imposed on the deformation  
 547 and on the growth tensor are such that  $k_0$  depends, through  $J$  and  $J_\gamma$ , only on the axial coordinate  
 548 and on time. Moreover, the same conclusion can be drawn for the diffusivity  $\mathfrak{d}_\alpha$ , which, with slight  
 549 abuse of notation, we express as  $\mathfrak{d}_\alpha(Z, t)$  from here on.

550 By following the same reasoning that has led to Equation (35), and noticing that the only  
 551 non-zero component of the mass flux  $\mathbf{Q}$  is the axial one, i.e.,  $\mathbf{Q}^Z = -\mathbf{K}^{ZZ} \frac{\partial \mathbf{p}}{\partial Z}$  with  $\mathbf{K}^{ZZ} =$   
 552  $Jk_0[\mathbf{C}^{-1}]^{ZZ} = k_0/(1 + u')$ , the continuity equation (26d) becomes

$$\frac{\partial^2 u}{\partial Z \partial t} - \frac{\partial}{\partial Z} \left( \frac{k_0}{1 + u'} \frac{\partial \mathbf{p}}{\partial Z} \right) = 0. \quad (36)$$

553 The equations for  $\mathbf{c}_p$  and  $\gamma$ , that is Equations (26a) and (26b), are scalar ODEs, and the fact  
 554 that  $\mathbf{c}_p$  and  $\gamma$  depend only of  $Z$  and  $t$  is consistent with the symmetry properties of all the terms  
 555 featuring in these equations. That said, a remark is in order for Equation (26b) to emphasise that  
 556 the considered benchmark problem remains three-dimensional in spite of the axial symmetry and  
 557 radial homogeneity that it enjoys. Indeed, looking at the source  $R_{\text{fp}}$  in Equation (27a), we notice  
 558 that the mechanotransduction term (i.e., the term between brackets in Equation (27a)) features  
 559 the trace of Cauchy stress tensor, which requires the evaluation of all the stress components, i.e.,  
 560 also of those in the radial and circumferential directions, these being non null because the cylinder  
 561 is laterally jacketed. Therefore, we conclude that, even though the cylinder used for our benchmark  
 562 problem is slender, with slenderness ratio  $2 \cdot 10^{-2}$  (see the geometric data in Table 1), the problem  
 563 itself necessitates to account for all the geometrical dimensions.

564 The last equation to consider is the balance law for  $\mathbf{c}_a$  (see Equation (26c)) in which the  
 565 non-standard mass flux  $\mathbf{Y}_\alpha$  features, at least in principle, all the coordinates (i.e., also the radial  
 566 and the circumferential coordinates) through the non-locality function  $\mathfrak{F}_\alpha(X, \tilde{X}, t) = \hat{\mathfrak{f}}_\alpha(\chi(X, t) -$   
 567  $\chi(\tilde{X}, t))$ . To maintain the axial symmetry of the problem and to eliminate the dependence of  
 568 the nutrients' mass flux on the radial and circumferential coordinates, two paths may be followed.  
 569 One is discussed in Section "Definition of the non-locality function" and, for consistency with the  
 570 symmetry requirements introduced so far, it imposes to rephrase the non-locality function as a  
 571 function of the axial coordinate only. However, another path —valid for the problem at hand—

572 could be to eliminate the dependence of the non-locality function on the radial and circumferential  
 573 coordinate by taking advantage of the slenderness of the cylinder. To this end, we write the non-  
 574 locality function as

$$\hat{f}_\alpha(x - \tilde{x}) = f_{0\alpha} \frac{1}{\|x - \tilde{x}\|^\alpha} = f_{0\alpha} \frac{1}{\|(z - \tilde{z})\mathbf{e}_z + \mathbf{r}_t\|^\alpha}, \quad (37)$$

575 where  $\mathbf{e}_z$  is the unit vector along which the cylinder's axis is directed,  $f_{0\alpha}$ , with  $\alpha \in ]0, 1[$ , is an  
 576  $\alpha$ -dependent coefficient to be individuated, and  $\mathbf{r}_t$  is a vector lying on the cross-section of the  
 577 cylinder. Next, we rescale the axial vector  $(z - \tilde{z})\mathbf{e}_z$  by the undeformed length of the cylinder, i.e.,  
 578  $2L_{\text{in}}$ , and the transverse vector  $\mathbf{r}_t$  by the cylinder diameter prior to deformation, i.e.,  $2R_{\text{in}}$ , so that  
 579 Equation (37) becomes

$$\hat{f}_\alpha(x - \tilde{x}) = f_{0\alpha} \frac{1}{\|2L_{\text{in}}\boldsymbol{\rho}_a + 2R_{\text{in}}\boldsymbol{\rho}_t\|^\alpha} = \frac{f_{0\alpha}}{(2L_{\text{in}})^\alpha} \frac{1}{\|\boldsymbol{\rho}_a + (R_{\text{in}}/L_{\text{in}})\boldsymbol{\rho}_t\|^\alpha}, \quad (38)$$

580 with  $\boldsymbol{\rho}_a = (z - \tilde{z})\mathbf{e}_z / (2L_{\text{in}})$  and  $\boldsymbol{\rho}_t := \mathbf{r}_t / (2R_{\text{in}})$ . Now, since the slenderness ratio  $R_{\text{in}}/L_{\text{in}}$  is  $2 \cdot 10^{-2}$ ,  
 581 we assume, within the first approximation, that the non-locality function can be truncated at the  
 582 zero-th order in the slenderness ratio, thereby taking the expression

$$\hat{f}_\alpha(x - \tilde{x}) \approx \frac{f_{0\alpha}}{(2L_{\text{in}})^\alpha} \frac{1}{\|\boldsymbol{\rho}_a\|^\alpha} = f_{0\alpha} \frac{1}{\|(z - \tilde{z})\mathbf{e}_z\|^\alpha} = f_{0\alpha} \frac{1}{|z - \tilde{z}|^\alpha}. \quad (39)$$

583 As discussed below, the coefficient  $f_{0\alpha}$  acquires the meaning of a normalisation factor.

## 584 7.2 Initial and boundary conditions

585 To solve Equations (26a)–(26e), we impose the same boundary and initial conditions used in  
 586 [101, 56]. Specifically, at the initial instant of time we consider a reference configuration being  
 587 characterised by the following relations

$$\chi^r(R, \Theta, Z, 0) = R, \quad \chi^\theta(R, \Theta, Z, 0) = \Theta, \quad \chi^z(R, \Theta, Z, 0) = Z, \quad (40)$$

588 where  $R \in [0, R_{\text{in}}[$ ,  $\Theta \in [0, 2\pi[$  and  $Z \in [-L_{\text{in}}, +L_{\text{in}}]$ , while  $R_{\text{in}}$  and  $2L_{\text{in}}$  denote the radius and  
 589 the length of the undeformed specimen. Besides, we enforce that, at  $t = 0$ , necrotic cells are  
 590 absent, i.e.,  $\mathbf{c}_p(R, \Theta, Z, 0) = 1$ , the fluid pressure is zero, i.e.,  $\mathbf{p}(R, \Theta, Z, 0) = 0$ , the nutrients' mass  
 591 fraction equals the environmental one, i.e.,  $\mathbf{c}_a(R, \Theta, Z, 0) = \mathbf{c}_{\text{env}} > 0$ , and the distribution of the  
 592 growth parameter is homogeneous and unitary, i.e.,  $\gamma(R, \Theta, Z, 0) = 1$ . In addition, we consider the  
 593 following boundary conditions

$$(-J\mathbf{p}\mathbf{g}^{-1}\mathbf{F}^{-\text{T}} + \mathbf{P}_{\text{sc}}) \cdot \mathbf{N}_A = \mathbf{0}, \quad \text{on } (\partial\mathcal{B})_{\text{Left}} \text{ and } (\partial\mathcal{B})_{\text{Right}}, \quad (41a)$$

$$(-\mathbf{K}\text{Grad}\mathbf{p}) \cdot \mathbf{N}_C = 0, \quad \text{on } (\partial\mathcal{B})_C, \quad (41b)$$

$$\mathbf{p} = 0, \quad \text{on } (\partial\mathcal{B})_{\text{Left}} \text{ and } (\partial\mathcal{B})_{\text{Right}}, \quad (41c)$$

$$\mathbf{c}_a = \mathbf{c}_{\text{env}}, \quad \text{on } (\partial\mathcal{B})_{\text{Left}} \text{ and } (\partial\mathcal{B})_{\text{Right}}, \quad (41d)$$

$$\mathbf{Y}_\alpha \cdot \mathbf{N}_C = 0, \quad \text{on } (\partial\mathcal{B})_C, \quad (41e)$$

594 where  $\mathbf{N}_A$  and  $\mathbf{N}_C$  are fields of unit vectors normal to  $(\partial\mathcal{B})_{\text{Left}} \cup (\partial\mathcal{B})_{\text{Right}}$  and to  $(\partial\mathcal{B})_C$ , respec-  
 595 tively, and  $\partial\mathcal{B} = (\partial\mathcal{B})_{\text{Left}} \cup (\partial\mathcal{B})_{\text{Right}} \cup (\partial\mathcal{B})_C$ . Specifically,  $(\partial\mathcal{B})_{\text{Left}}$  and  $(\partial\mathcal{B})_{\text{Right}}$  are the left  
 596 and the right surfaces at the extremities of  $\mathcal{B}$ , and  $(\partial\mathcal{B})_C$  is the lateral boundary.

### 597 7.3 Definition of the non-locality function

598 A classical approach for defining  $\hat{f}_\alpha$  is to adopt a power-law that decays in space. To our knowledge,  
 599 this is customary for problems that are *a priori* formulated as one-dimensional and in which  $\hat{f}_\alpha(x-\tilde{x})$   
 600 is assumed to be proportional to the reciprocal of  $|x-\tilde{x}|^\alpha$ , with  $x$  and  $\tilde{x}$  being points of the real  
 601 line or of an interval of finite length [112, 111, 108, 22, 105]. This choice permits to “import”,  
 602 with slight modifications, the definitions of the fractional derivatives in time (see e.g. [9]) to the  
 603 fractional differentiation in space. However, in some situations it is necessary to assess an *a priori*  
 604 relationship between the dimensionality of the problem under study and the non-locality that *must*  
 605 —or *may*— be resolved, once the dimensionality has been settled. Indeed, in a three-dimensional  
 606 problem endowed with the symmetry and homogeneity properties we are dealing with, the only  
 607 non-zero partial derivative of the concentration is the one along the axial direction. In such a  
 608 situation, the axial mass flux reads

$$[\mathbf{y}_\alpha(x, t)]^z = -\varrho_f \int_{\mathcal{B}_t} \hat{f}_\alpha(x - \tilde{x}) \mathfrak{d}_\alpha(\tilde{z}, t) \partial_{\tilde{z}} c_a(\tilde{z}, t) \mathrm{d}v(\tilde{x}), \quad (42)$$

609 whereas the radial and the circumferential components of the flux are zero. Note that we are using  
 610 here the customary formalism for cylindrical coordinates, so that  $\tilde{x} = (\tilde{r}, \tilde{\vartheta}, \tilde{z})$ . As anticipated  
 611 before, the expression for  $[\mathbf{y}_\alpha(x, t)]^z$  reminds the definition of fractional gradient given in [113],  
 612 with the difference that a volume integral is used in (42) and that all the components of  $x - \tilde{x}$  are  
 613 considered.

614 In spite of the fact that the problem is one-dimensional from the point of view of its symmetries,  
 615 the axial flux is still determined by an integration over the three-dimensional region  $\mathcal{B}_t$ , and  $\hat{f}_\alpha(x-\tilde{x})$   
 616 describes, as it stands, a non-locality in three dimensions (trivially, because  $x - \tilde{x}$  is a vector of  
 617 a three-dimensional vector space). Therefore, the component of  $(x - \tilde{x})$  along the radial or the  
 618 circumferential direction will influence the axial mass flux, even though the problem was claimed  
 619 to enjoy axial symmetry and to be independent of the radial coordinate. This result, however, may  
 620 be physically unsound. Indeed, one would expect non-locality to be coherent with the symmetries  
 621 of the problem, even though the integral of Equation (42) is over the whole configuration  $\mathcal{B}_t$ ,  
 622 thereby maintaining the physical dimensionality of the problem itself.

623 To address this issue, we need to take into account how the symmetries of the problem under  
 624 investigation influence the non-locality in the relationship between  $\mathbf{y}_\alpha$  and  $c_a$ . Consequently, the  
 625 non-locality function  $\hat{f}_\alpha$  in Equation (42) is re-defined as

$$\hat{f}_\alpha(x - \tilde{x}) := \hat{h}_\alpha(z - \tilde{z}) = \frac{1}{\mathcal{N}(\alpha)} \frac{1}{|z - \tilde{z}|^\alpha}, \quad \alpha \in ]0, 1[, \quad (43)$$

626 where  $\mathcal{N}(\alpha)$  is a normalisation factor to be determined. From Equations (42) and (43), we notice  
 627 that the physical dimensions of the fractional diffusivity,  $\mathfrak{d}_\alpha$ , are  $L^{1+\alpha}T^{-1}$ , where  $L$  and  $T$  stand  
 628 for the characteristic “length” and the characteristic “time” of the non-local diffusion process,  
 629 respectively. Thus, when  $\alpha$  tends to 1 (from below), we recover the physical dimensions of the  
 630 standard diffusivity.

631 By substituting Equation (43) into Equation (42), and recalling that  $\mathcal{B}_t = \mathcal{C}_R \times ]-\ell(t), +\ell(t)[$   
 632 (where  $\mathcal{C}_R$  is the cross-section of the cylinder and  $2\ell(t)$  is its variable axial length), we obtain the  
 633 much simpler expression

$$[\mathbf{y}_\alpha(x, t)]^z \equiv y_\alpha^z(z, t) = -\frac{\varrho_f \pi R_{\text{in}}^2}{\mathcal{N}(\alpha)} \int_{-\ell(t)}^{+\ell(t)} \frac{1}{|z - \tilde{z}|^\alpha} \mathfrak{d}_\alpha(\tilde{z}, t) \partial_{\tilde{z}} c_a(\tilde{z}, t) \mathrm{d}\tilde{z}. \quad (44)$$

634 For the Equation (44) to be physically sound, it has to return the axial component of the standard  
635 mass flux vector in the limit  $\alpha \rightarrow 1^-$ . Unfortunately, proving this result for problems defined over  
636 bounded domains is not possible without knowing  $c_a$ . On the contrary, this difficulty does not arise  
637 in problems defined over unbounded domains, because, with the aid of the Fourier transform, it is  
638 possible to do the following reasoning:

- 639 • Introduce the auxiliary notation  $\psi_\alpha^z(\tilde{z}, t) := -\varrho_f \mathfrak{d}_\alpha(\tilde{z}, t) \partial_z c_a(\tilde{z}, t)$ , and assume to prolong  
640  $y_\alpha^z(z, t)$  to the whole real line, so that Equation (44) becomes

$$\begin{aligned} y_\alpha^z(z, t) &= -\frac{\varrho_f \pi R_{\text{in}}^2}{\mathcal{N}(\alpha)} \int_{-\infty}^{+\infty} \frac{1}{|z - \tilde{z}|^\alpha} \mathfrak{d}_\alpha(\tilde{z}, t) \partial_z c_a(\tilde{z}, t) d\tilde{z} \\ &= \pi R_{\text{in}}^2 \int_{-\infty}^{+\infty} \hat{\mathfrak{h}}_\alpha(z - \tilde{z}) \psi_\alpha^z(\tilde{z}, t) d\tilde{z} \\ &= \pi R_{\text{in}}^2 [\hat{\mathfrak{h}}_\alpha * \psi_\alpha^z(\cdot, t)](z), \end{aligned} \quad (45)$$

641 thereby expressing  $y_\alpha^z(z, t)$  as the convolution product between  $\hat{\mathfrak{h}}_\alpha$  and  $\psi_\alpha^z(\cdot, t)$ .

- 642 • Compute the Fourier transform of  $y_\alpha^z(z, t)$  as written in Equation (45), i.e.,

$$\begin{aligned} \mathcal{F}[y_\alpha^z(\cdot, t)](\xi) &:= \int_{-\infty}^{+\infty} y_\alpha^z(z, t) \exp(-i\xi z) dz \\ &= \pi R_{\text{in}}^2 \mathcal{F}[\hat{\mathfrak{h}}_\alpha](\xi) \mathcal{F}[\psi_\alpha^z(\cdot, t)](\xi) \\ &= \pi R_{\text{in}}^2 \frac{2\Gamma(1 - \alpha)}{\mathcal{N}(\alpha)} \sin\left(\frac{\alpha\pi}{2}\right) |\xi|^{\alpha-1} \mathcal{F}[\psi_\alpha^z(\cdot, t)](\xi), \end{aligned} \quad (46)$$

643 where  $\xi \in \mathbb{R} \setminus \{0\}$  is the wave number,  $\Gamma(\cdot)$  is the Euler Gamma function and we used the  
644 Fourier transform of  $\hat{\mathfrak{h}}_\alpha$ , i.e.,

$$\mathcal{F}[\hat{\mathfrak{h}}_\alpha](\xi) = \frac{2\Gamma(1 - \alpha)}{\mathcal{N}(\alpha)} \sin\left(\frac{\alpha\pi}{2}\right) |\xi|^{\alpha-1}. \quad (47)$$

645 Since  $\mathcal{F}[y_\alpha^z(\cdot, t)](\xi)$  is proportional to the product of  $\mathcal{F}[\hat{\mathfrak{h}}_\alpha](\xi)$  and  $\mathcal{F}[\psi_\alpha^z(\cdot, t)](\xi)$ , one can  
646 identify the non-local contribution of the mass flux with  $\mathcal{F}[\hat{\mathfrak{h}}_\alpha](\xi)$ , given in Equation (47).

647 Note that, if  $\mathfrak{d}_\alpha(z, t)$  and  $c_a(z, t)$  are both assumed to be even with respect to  $z = 0$  — an  
648 assumption that is consistent with the hypothesis, done later, that the considered problem  
649 is symmetric with respect to  $z = 0$  —,  $\mathcal{F}[y_\alpha^z(\cdot, t)](\xi)$  can be prolonged to  $\xi = 0$  and is null for  
650 this value. To see this, we first rewrite  $\mathcal{F}[\psi_\alpha^z(\cdot, t)](\xi)$  as

$$\mathcal{F}[\psi_\alpha^z(\cdot, t)](\xi) = -\varrho_f \int_{-\infty}^{+\infty} \mathfrak{d}_\alpha(z, t) \partial_z c_a(z, t) \exp(-i\xi z) dz. \quad (48)$$

651 Then, we notice that  $\mathcal{F}[\psi_\alpha^z(\cdot, t)](0)$  is zero, because  $\mathfrak{d}_\alpha(z, t)$  is even and  $\partial_z c_a(z, t)$  is odd  
652 with respect to  $z = 0$  for all times. Moreover, because of this result, it also holds that  
653  $\lim_{\xi \rightarrow 0} |\xi|^{\alpha-1} \mathcal{F}[\psi_\alpha^z(\cdot, t)](\xi) = 0$ , and, consequently,  $\lim_{\xi \rightarrow 0} \mathcal{F}[y_\alpha^z(\cdot, t)](\xi) = 0$  too.



654 • Compute the limit of  $\mathcal{F}[y_\alpha^z(\cdot, t)](\xi)$  for  $\alpha \rightarrow 1^-$ , and find  $\mathcal{N}(\alpha)$  such that

$$\begin{aligned} \lim_{\alpha \rightarrow 1^-} \mathcal{F}[y_\alpha^z(\cdot, t)](\xi) &= \lim_{\alpha \rightarrow 1^-} \mathcal{F}[\psi_\alpha^z(\cdot, t)](\xi) \\ &= \mathcal{F}[-\varrho_f \mathfrak{d}_1(\cdot, t) \partial_z c_a(\cdot, t)](\xi), \end{aligned} \quad (49)$$

655 with  $\mathfrak{d}_1(\tilde{z}, t) := \lim_{\alpha \rightarrow 1^-} \mathfrak{d}_\alpha(\tilde{z}, t)$ . We emphasise that this limit is taken uniformly with respect  
656 to the pairs  $(\tilde{z}, t)$  and, in particular, looking at Equation (24), it turns out to be uniform  
657 with respect to the motion, so that it is intended as

$$\begin{aligned} \lim_{\alpha \rightarrow 1^-} \mathfrak{d}_\alpha(\tilde{z}, t) &= \lim_{\alpha \rightarrow 1^-} \mathfrak{d}_\alpha(\chi^z(\tilde{X}, t), t) = \frac{J(\tilde{X}, t) - J_\gamma(\tilde{X}, t)\Phi_{s\nu}}{J(\tilde{X}, t)} \lim_{\alpha \rightarrow 1^-} \mathfrak{d}_{R\alpha} \\ &= \frac{J(\tilde{X}, t) - J_\gamma(\tilde{X}, t)\Phi_{s\nu}}{J(\tilde{X}, t)} \mathfrak{d}_{R1}, \end{aligned} \quad (50)$$

658 where, in our model,  $\mathfrak{d}_{R1}$  is a constant having the physical dimensions of a standard diffusivity  
659 coefficient. In particular, to meet this requirement, we choose  $\mathfrak{d}_{R\alpha}$  as

$$\mathfrak{d}_{R\alpha} := d_R L^{\alpha-1}, \quad (51)$$

660 with  $d_R$  being a constant reference value for the standard diffusivity coefficient [13], so that  
661  $\mathfrak{d}_{R1} = d_R$ .

662 One possible way to comply with Equation (49) is that  $\mathcal{N}(\alpha)$  satisfies the relation

$$\lim_{\alpha \rightarrow 1^-} \frac{2\Gamma(1-\alpha)\pi R_{\text{in}}^2}{\mathcal{N}(\alpha)} = 1. \quad (52)$$

663 Then, for Equation (44) to be (up to the diffusivity  $\mathfrak{d}_\alpha$ ) Caputo's symmetrised fractional derivative  
664 of the mass fraction,  $c_a$ , which is defined over the interval  $] -\ell(t), +\ell(t)[$ , we choose the stronger  
665 condition

$$\mathcal{N}(\alpha) = 2\Gamma(1-\alpha)\pi R_{\text{in}}^2, \quad \alpha \in ]0, 1[. \quad (53)$$

666 Clearly, Equation (53) represents a “guess”, because we are unable to compute directly the nor-  
667 malisation factor for a bounded interval. Nevertheless, plugging Equation (53) into Equation (44)  
668 yields

$$y_\alpha^z(z, t) = -\frac{\varrho_f}{2\Gamma(1-\alpha)} \int_{-\ell(t)}^{+\ell(t)} \frac{1}{|z - \tilde{z}|^\alpha} \mathfrak{d}_\alpha(\tilde{z}, t) \partial_{\tilde{z}} c_a(\tilde{z}, t) d\tilde{z}, \quad (54)$$

669 which, apart from the spatial dependence of the fractional diffusivity  $\mathfrak{d}_\alpha(\tilde{z}, t)$ , coincides with the  
670 definition of fractional mass flux in one dimension used by other Authors, see for instance [89, 35]  
671 and the references therein. Furthermore, in the case in which the fractional diffusivity can be  
672 factorised outside the integral operator, e.g. by setting  $\mathfrak{d}_\alpha(\tilde{z}, t) = \mathfrak{d}_{0\alpha}$ , the axial mass flux becomes  
673 proportional to the symmetrised Caputo fractional derivative of order  $\alpha$  of  $c_a$  [9].

674 **Remark 3 ((On the normalisation factor))** We notice that, apart from the presence of the  
675 area of the cylinder's cross-section  $|\mathcal{C}_R| = \pi R_{\text{in}}^2$ , the expression of the normalisation factor  $\mathcal{N}(\alpha)$   
676 given in Equation (53) coincides with the one used in other works (see e.g. [112, 11, 22]). Never-  
677 theless, by looking at Equation (46), one can see that other definitions of the normalisation factor  
678 can be employed which satisfy the condition of Equation (49). Indeed, if the limit in Equation (52)  
679 is rephrased as

$$\lim_{\alpha \rightarrow 1^-} \frac{2\Gamma(1-\alpha) \sin(\alpha\pi/2) \pi R_{\text{in}}^2}{\hat{\mathcal{N}}(\alpha)} = 1, \quad (55)$$

680 where  $\hat{\mathcal{N}}(\alpha)$  is the new normalisation factor sought for, then, upon following the reasoning leading  
681 to Equation (53), one can take  $\hat{\mathcal{N}}(\alpha)$  as

$$\hat{\mathcal{N}}(\alpha) := 2\Gamma(1-\alpha) \sin(\alpha\pi/2) \pi R_{\text{in}}^2, \quad (56)$$

682 thereby automatically satisfying Equation (55). Then, by using  $\hat{\mathcal{N}}(\alpha)$  in Equation (44) in lieu of  
683  $\mathcal{N}(\alpha)$ , the axial mass flux can be written as

$$\begin{aligned} \hat{y}_\alpha^z(z, t) &= -\frac{\varrho_f}{2\Gamma(1-\alpha) \sin(\alpha\pi/2)} \int_{-\ell(t)}^{+\ell(t)} \frac{1}{|z-\tilde{z}|^\alpha} \mathfrak{d}_\alpha(\tilde{z}, t) \partial_{\tilde{z}} c_a(\tilde{z}, t) d\tilde{z} \\ &= \mathcal{I}_{-\ell(t), +\ell(t)}^{1-\alpha} [-\varrho_f \mathfrak{d}_\alpha \partial_{\tilde{z}} c_a](z, t), \end{aligned} \quad (57)$$

684 where  $\mathcal{I}_{-\ell(t), +\ell(t)}^{1-\alpha} [-\varrho_f \mathfrak{d}_\alpha \partial_{\tilde{z}} c_a]$  is the one-dimensional Riesz potential of  $-\varrho_f \mathfrak{d}_\alpha \partial_{\tilde{z}} c_a$ , but with inte-  
685 gration limits  $\pm\ell(t)$  instead of  $\pm\infty$  (see [104] page 223). For this reason, one may refer to Equation  
686 (57) as a “truncated” Riesz potential [38].

687 At this point, two comments are in order. First, we note that, for  $\alpha \rightarrow 1^-$ , both choices of the  
688 normalisation factor lead to the same result and, consequently, the mass flux obtained for  $\alpha \rightarrow 1^-$   
689 is the same in both formulations. However, something different occurs for  $\alpha \rightarrow 0^+$ . Indeed, by  
690 looking at Equation (46), if the normalisation factor  $\mathcal{N}(\alpha)$  is used, we obtain, for  $\xi \neq 0$ , that

$$\lim_{\alpha \rightarrow 0^+} \mathcal{F}[y_\alpha^z(\cdot, t)](\xi) = 0, \quad (58)$$

691 which suggests that the flux of the species is null for  $\alpha \rightarrow 0^+$ . On the contrary, if in Equation (46)  
692  $\mathcal{N}(\alpha)$  is replaced with  $\hat{\mathcal{N}}(\alpha)$ , one obtains, for  $\xi \neq 0$ ,

$$\lim_{\alpha \rightarrow 0^+} \mathcal{F}[\hat{y}_\alpha^z(\cdot, t)](\xi) = |\xi|^{-1} \mathcal{F}[-\varrho_f \mathfrak{d}_0(\cdot, t) \partial_z c_a(\cdot, t)](\xi), \quad (59)$$

693 with  $\mathfrak{d}_0 = \lim_{\alpha \rightarrow 0^+} \mathfrak{d}_\alpha$ , thereby implying, in general, a non-zero flux. In view of the above results and  
694 of the normalisation factor used by other Authors [89, 35, 11, 105], we prefer to employ  $\mathcal{N}(\alpha)$  as  
695 normalisation factor in the remainder of this work. Besides, in this way, the model is able to account  
696 for a wider range of diffusion situations, from no diffusion to standard diffusion. Nevertheless, for  
697 completeness in our study, in Section “Results and discussion”, we provide a comparison between  
698 the approach involving  $\mathcal{N}(\alpha)$  and that involving  $\hat{\mathcal{N}}(\alpha)$ .

699 Now, the restrictions imposed on the motion imply that the only component of interest of the  
700 deformation gradient tensor is given by  $[\mathbf{F}(X, t)]^z_Z = 1 + u'(Z, t)$ . Thus, by taking into account  
701 Equation (25), the material fractional diffusivity tensor can be rephrased as follows

$$[\mathfrak{D}_\alpha(X, \tilde{X}, t)]^{ZZ} = \mathfrak{D}_{R\alpha} \frac{1 + u'(\tilde{Z}, t) - J_\gamma(\tilde{Z}, t) \Phi_{s\nu}}{[1 + u'(Z, t)][1 + u'(\tilde{Z}, t)]}, \quad (60)$$

702 whereas the definition (43) implies that  $\mathfrak{F}_\alpha$ , given in Equation (22b), can be rephrased as a function  
 703 of  $Z$ ,  $\tilde{Z}$  and  $t$ , i.e.,

$$\mathfrak{F}_\alpha(X, \tilde{X}, t) = \mathfrak{H}_\alpha(Z, \tilde{Z}, t) = \frac{1}{2\Gamma(1-\alpha)\pi R_{\text{in}}^2} \frac{1}{|Z + u(Z, t) - \tilde{Z} - u(\tilde{Z}, t)|^\alpha}, \quad \alpha \in ]0, 1[. \quad (61)$$

704 Finally, by substituting Equation (60) into Equation (23b), and taking into account relation (22b),  
 705 the only non-zero component of the material fractional mass flux vector,  $\mathbf{Y}_\alpha$ , is the one along the  
 706 axial direction, and represents the backward Piola transform of Equation (44), i.e.,

$$Y_\alpha^Z(Z, t) = -\frac{\varrho_f}{2\Gamma(1-\alpha)} \int_{-L_{\text{in}}}^{+L_{\text{in}}} \mathfrak{D}_{R\alpha} \frac{[1 + u'(\tilde{Z}, t) - J_\gamma(\tilde{Z}, t)\Phi_{s\nu}]}{|Z + u(Z, t) - \tilde{Z} - u(\tilde{Z}, t)|^\alpha} \frac{\mathbf{c}'_a(\tilde{Z}, t)}{[1 + u'(\tilde{Z}, t)]} d\tilde{Z}. \quad (62)$$

707 Looking at Equations (61) and (62), we remark that, in contrast to what is usually assumed in the  
 708 “standard” setting of Fractional Calculus, both  $\mathfrak{H}_\alpha$  and  $Y_\alpha^Z$  depend on the displacement field, rather  
 709 than depending on the difference between  $Z$  and  $\tilde{Z}$ , only. As anticipated in the Introduction, this  
 710 result is one of the most relevant novelties of our work, as it prescribes that the non-locality evolves  
 711 with the change of configuration of the system. Moreover, since in our framework the displacement  
 712 is driven by growth (even though  $u$  and  $\gamma$  are formally independent variables), we conclude that  
 713 the non-locality of the problem is related also to the variation of the tissue’s internal structure, as  
 714 modelled by  $\gamma$ .

## 715 8 Results and discussion

716 In this section, we study the impact of the non-local diffusion of nutrients on the benchmark  
 717 problem specified above. For this scope, we distinguish between two mathematical models, both  
 718 characterised by Equations (26a)–(26e). The first model, referred to as *fractional model*, describes  
 719 the growth of the considered avascular tumour in the case in which the diffusion of the nutrients is  
 720 governed by the non-local constitutive law (62). The second model, denominated *standard model*,  
 721 describes the growth of the tumour by employing the same governing equations (26a)–(26e), with  
 722 the only difference being that the nutrients’ diffusive mass flux vector is expressed by standard  
 723 Fick’s law, i.e.,

$$\mathbf{Y}_{\text{std}}(X, t) = -\varrho_f \mathbf{D}(X, t) \text{Grad} \mathbf{c}_a(X, t), \quad (63)$$

724 where “std” stands for “standard”, and  $\mathbf{D}$  is the *material diffusivity tensor*, given by [101, 56]

$$\mathbf{D}(X, t) = (J(X, t) - J_\gamma(X, t)\Phi_{s\nu}) d_R \mathbf{C}^{-1}(X, t). \quad (64)$$

725 We notice that both models, i.e., the fractional and the standard one, share the same set of param-  
 726 eters except for the reference diffusivities  $\mathfrak{D}_{R\alpha}$  and  $d_R$ . Note also that Equation (64) can be obtained  
 727 from (25) by setting  $\tilde{X} = X$  and then taking the limit for  $\alpha \rightarrow 1^-$ , i.e.,  $\lim_{\alpha \rightarrow 1^-} \mathfrak{D}_\alpha(X, X, t) =$   
 728  $\mathbf{D}(X, t)$ .

729 For the purposes of our work, one should not fix  $\mathfrak{D}_{R\alpha}$  independently of  $d_R$ . Indeed, in order to  
 730 compare the results of the non-local model with those of the local one,  $\mathfrak{D}_{R\alpha}$  must depend on  $d_R$   
 731 in such a way that it tends to  $d_R$  in the limit  $\alpha \rightarrow 1^-$ . For this reason, and taking into account

732 that there exist several experimental works in which the standard diffusivity of species in biological  
733 tissues has been measured (see e.g. [62, 59]), we use for  $\mathfrak{D}_{R\alpha}$  the definition given in Equation (51),  
734 and we set  $L = 2L_{\text{in}}$ . In Table 1, we provide the list of all the parameters used in our simulations.  
735 We remark that, due to the symmetries of the benchmark problem studied in this work, in the  
736 following we report the profile of the main quantities of interest restricted to half of the domain,  
737 i.e.,  $[0, L_{\text{in}}]$ .

Table 1: List of parameters used in the numerical simulations.

Parameter	Unit	Value	Equation	Reference
$L_{\text{in}}$	cm	0.500	(44)	[101]
$R_{\text{in}}$	cm	$1.000 \cdot 10^{-2}$	(62)	[101]
$\lambda$	Pa	$1.333 \cdot 10^4$	(12)	[111]
$\mu$	Pa	$1.999 \cdot 10^4$	(12)	[111]
$k_{\text{R}}$	$\text{m}^2/(\text{Pa}\cdot\text{s})$	$4.875 \cdot 10^{-13}$	(15)	[62]
$m_0$	—	0.0848	(15)	[62]
$m_1$	—	4.638	(15)	[62]
$d_{\text{R}}$	$\text{m}^2/\text{s}$	$3.200 \cdot 10^{-9}$	(51)	[107]
$\zeta_{\text{fp}}$	$\text{kg}/(\text{m}^3\text{s})$	$1.343 \cdot 10^{-3}$	(27a)	[25]
$\zeta_{\text{nf}}$	$\text{kg}/(\text{m}^3\text{s})$	$1.150 \cdot 10^{-5}$	(27b)	[25]
$\zeta_{\text{cp}}$	$\text{kg}/(\text{m}^3\text{s})$	$3.000 \cdot 10^{-4}$	(27c)	[23, 24]
$\zeta_{\text{pn}}$	$\text{kg}/(\text{m}^3\text{s})$	$1.500 \cdot 10^{-3}$	(27d)	[25]
$\mathfrak{c}_{\text{cr}}$	—	$1.000 \cdot 10^{-3}$	(27a)	[101]
$\mathfrak{c}_{\text{env}}$	—	$7.000 \cdot 10^{-3}$	(27a)	[101]
$\mathfrak{c}_0$	—	$1.000 \cdot 10^{-2}$	(27c)	This work
$\delta_1$	—	$7.138 \cdot 10^{-1}$	(27a)	[80]
$\delta_2$	Pa	$1.541 \cdot 10^3$	(27a)	[80]
$\Phi_{\text{sv}}$	—	0.8	(5a)	[101]
$\varrho_{\text{s}}$	$\text{kg}/\text{m}^3$	1000	(2)	[101]
$\varrho_{\text{f}}$	$\text{kg}/\text{m}^3$	1000	(2)	[101]

738 To start with, in Fig. 1, we report the spatial profile of the nutrients' mass fraction  $\mathfrak{c}_a(Z, t)$ .  
739 Specifically, in the left panel of Fig. 1, we present the results of our simulations for  $\alpha = 0.1$  (dashed  
740 line) and  $\alpha = 0.9$  (solid line), and for different times. As shown in this plot, the parameter  $\alpha$  permits  
741 to control how the nutrients diffuse into the tumour from the axial boundaries (i.e., the terminal  
742 cross sections  $Z = \pm L_{\text{in}}$ ). In particular, for  $\alpha = 0.1$  the diffusion of the nutrients is constrained to  
743 the tumour's axial boundary, i.e., close to  $Z = \pm L_{\text{in}}$ , so that their mass fraction is dramatically  
744 reduced in the internal points of the specimen. In such a situation, the proliferating cells consume  
745 the nutrients that are already present in the tissue, without the replenishment needed to continue  
746 their proliferation. On the contrary, for  $\alpha = 0.9$ , the nutrients are able to diffuse towards the centre  
747 of the tumour, so that their consumption is less localised. For clarity, in the plot we prefer to show  
748 only the curves corresponding to  $\alpha = 0.1$  and  $\alpha = 0.9$ . For any other value of  $\alpha \in ]0.1, 0.9[$ , the  
749 model is able to describe different diffusion profiles ranging between the ones obtained for  $\alpha = 0.1$   
750 and for  $\alpha = 0.9$ . To us, an interesting feature of the curves corresponding to  $\alpha = 0.1$  is that,  
751 depending on the point  $Z$  at which the nutrients' mass fraction is observed, the trend of these

752 curves exhibits a different monotonicity in time. Indeed, the nutrients' mass fraction decreases in  
753 time close to the boundary  $Z = L_{\text{in}}$ , whereas it increases towards the tumour's centre. Furthermore,  
754 in the panel on the right of Fig. 1, we compare, for different values of  $\alpha$ , the results obtained with  
755 the fractional model with those obtained with the standard model at time  $t = 20$  d. Specifically, for  
756  $\alpha$  close to 0, there is almost no diffusion, while, when  $\alpha$  is close to 1, the fractional model conducts  
757 to the standard one, as evidenced by our previous calculations (see Equation (46)).

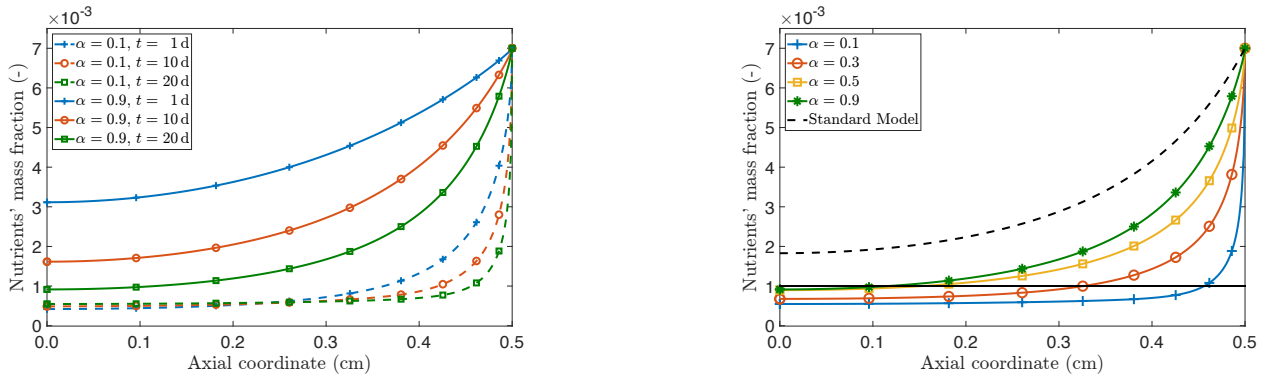


Figure 1: Spatial profile of the nutrients' mass fraction  $c_a(Z, t)$  for different values of  $\alpha$  and at different times (panel on the left), and comparison of the results obtained with the fractional and the standard model at time  $t = 20$  d (panel on the right).

758 As shown in Fig. 2, the non-local way in which the nutrients diffuse into the tissue affects  
759 the manner in which the tumour grows. By increasing  $\alpha$  and, thus, enhancing diffusion, one also  
760 increases the availability of the nutrients in the tumour, thereby boosting its growth. On the  
761 other hand, for  $\alpha = 0.1$ , the displacement is hindered and its highest values are attained in a  
762 neighbourhood of  $Z = L_{\text{in}}$ . Indeed, this is where the nutrients enter the tumour and their mass  
763 fraction still remains high enough to trigger growth, so that the magnitude of the displacement in  
764 this region of the tumour is higher than elsewhere. However, moving towards the interior of the  
765 tumour, the fact that the nutrients' concentration is below the critical threshold brings growth to  
766 a stop, thereby considerably reducing the magnitude of the displacement. This behaviour shows  
767 that also the monotonicity in time of the displacement curves depends on the point  $Z$  at which  
768 they are reckoned. More in detail, the reduction of the displacement in the interior of the tumour  
769 may be due to the loss of mass caused by the lack of nutrients, which implies that the proliferating  
770 cells start to die, and a region of necrotic cells comes into sight. This behaviour becomes even more  
771 evident by looking at the left panel of Fig. 3. Moreover, comparing the right panels of Fig. 1 and  
772 Fig. 3, we notice that the part of the domain in which the necrotic cells appear coincides with the  
773 one in which the nutrients fall below the critical value  $c_{\text{cr}}$ , represented with the solid horizontal line  
774 in the right panel of Fig. 1. By referring to Equation (27d), when  $c_a < c_{\text{cr}}$ , the rate of mass  $R_{\text{pn}}$   
775 becomes active and, therefore, the proliferating cells change into necrotic cells.

776 To continue our analysis, we refer to Fig. 4, where we plot the growth parameter  $\gamma$ . By focusing  
777 on the panel on the left, we notice, for  $\alpha = 0.1$ , a localisation of the variation of the growth  
778 parameter near the boundary  $Z = L_{\text{in}}$  for increasing time, whereas, for  $\alpha = 0.9$ , the variation of  
779  $\gamma$  is more uniformly distributed in the whole domain. Besides, for  $\alpha = 0.1$ ,  $\gamma$  is greater than one  
780 for all  $Z \in [0, L_{\text{in}}]$  and for all  $t$ , even though this is difficult to be observed with the unaided eye.

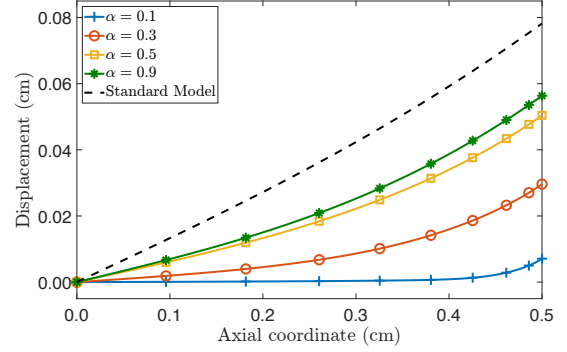
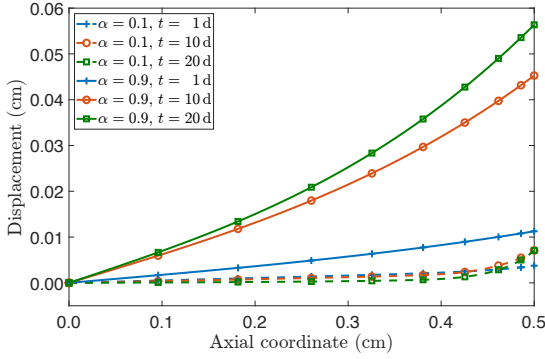


Figure 2: Spatial profile of the axial displacement  $u(Z,t)$  for different values of  $\alpha$  and at different times (panel on the left), and comparison of the results obtained with the fractional and the standard model at time  $t = 20$  d (panel on the right).

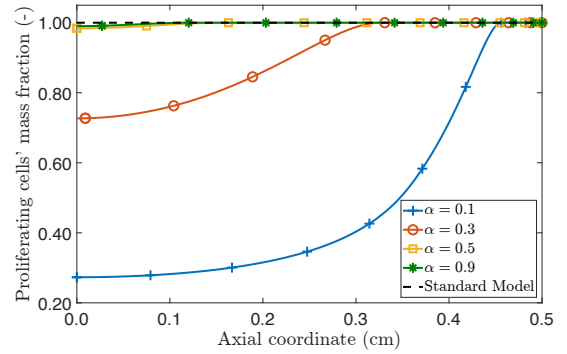
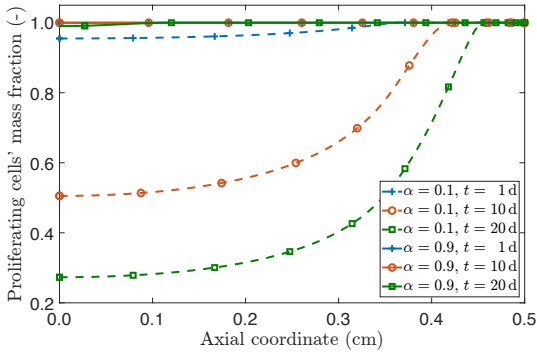


Figure 3: Spatial profile of the proliferating cells' mass fraction  $c_p(Z,t)$  for different values of  $\alpha$  and at different times (panel on the left), and comparison of the results obtained with the fractional and the standard model at time  $t = 20$  d (panel on the right).

781 This is because, although for  $t \geq 1$  d the mass fraction of the nutrients is above the threshold  
782 value  $c_{cr}$  mostly near the boundary (see the left panel of Fig. 1), the inner region has undergone  
783 a growth process at earlier times. Indeed, since the condition  $c_a(Z,0) \equiv c_{env} > c_{cr}$  is respected,  
784 the mass rate  $R_{fp}$  is greater than zero, and we can conclude that, from the very beginning, the cell  
785 proliferation is promoted until the nutrients' concentration falls below its critical value. Note also  
786 that this is accelerated when  $\alpha$  is near zero because of the slow pace with which the nutrients are  
787 refilled. At this point, the proliferating cells abruptly die, thereby turning into necrotic cells, and  
788 go into the fluid (see the definition of  $R_{nf}$ ), which results in a loss of mass. For  $\alpha = 0.9$ , instead, it  
789 is visible also with the naked eye that  $\gamma$  is greater than unity everywhere in  $[0, L_{in}]$  and for all the  
790 considered times. Finally, as noticed for the nutrients' mass fraction and for the displacement, also  
791 the monotonicity in time of the trend of the growth parameter depends, for  $\alpha = 0.1$ , on the point  
792  $Z$  at which  $\gamma$  is observed. Indeed,  $\gamma$  is monotonically increasing in time for  $Z$  close to  $Z = L_{in}$ , and  
793 monotonically decreasing for  $Z$  "moving" towards the centre of the tumour.

794 Now, we report the evolution of the pressure,  $p$ , in Fig. 5. For both the standard and the  
795 fractional model, when  $\alpha$  is close to 1, the pressure of the interstitial fluid decreases, taking negative

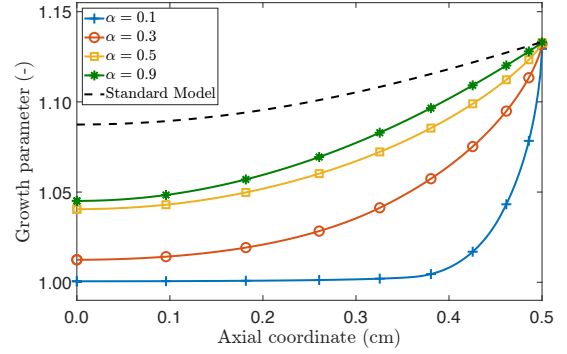
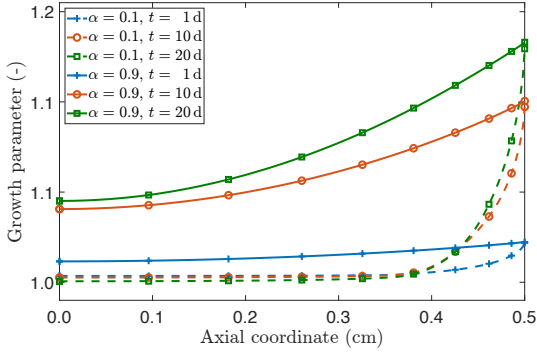


Figure 4: Spatial profile of the growth parameter  $\gamma(Z, t)$  for different values of  $\alpha$  and at different times (panel on the left), and comparison of the results obtained with the fractional and the standard model at time  $t = 20$  d (panel on the right).

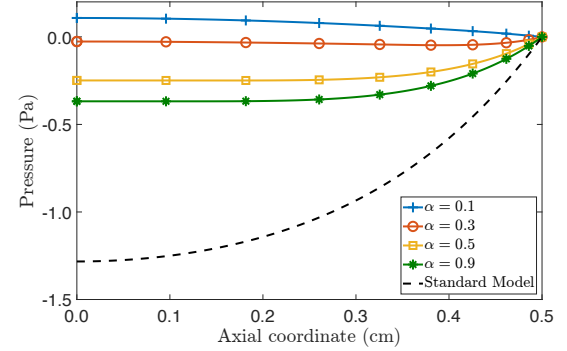
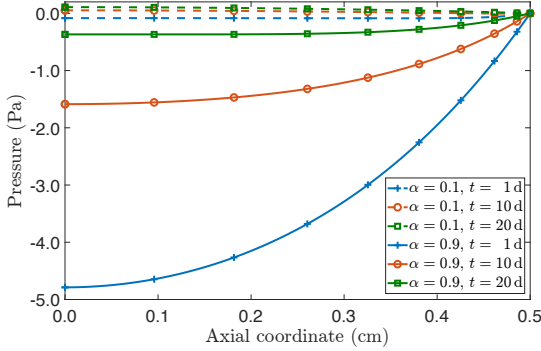


Figure 5: Spatial profile of the pressure  $\mathbf{p}(Z, t)$  for different values of  $\alpha$  and at different times (panel on the left), and comparison of the results obtained by the fractional and the standard model at time  $t = 20$  d (panel on the right).

796 values, from the free boundary towards the tumour's centre. However, for  $\alpha$  tending towards 0 from  
797 above, the pressure in the interior of the tumour tends to become positive. To explain this event,  
798 we notice that the proliferating cells absorb fluid from the surrounding environment to fuel their  
799 growth, which is possible because the fluid flows towards the tumour's interior. However, due to  
800 an over-consumption of nutrients, the level of those drastically decreases in the innermost zone  
801 of the tumour. This situation, as evidenced in our simulations (see Fig. 4), creates a layer of  
802 proliferating cells near the outer surface (i.e., the cross section  $Z = L_{\text{in}}$ ), and a region of necrotic  
803 cells at the centre of the tumour. By looking at Equation (27b), in this circumstance, the necrotic  
804 cells dissolve into the fluid with rate  $\zeta_{\text{nf}}$ , thereby increasing its pressure, which, in turn, generates  
805 an outward flux (i.e., a flux in the direction opposite to the fluid flow). This sequence of events,  
806 which are consistent with the biological foundations of nutrient diffusion and necrosis in a tumour  
807 as explained in [77], arises in the model thanks to the non-local approach presented in this work.  
808 That is, the non-locality parameter  $\alpha$  is responsible for this picture and, thus, through its inclusion,  
809 the fractional model is able to reproduce a scenario that was not initially considered in the model.  
810 On the contrary, as the results show, this behaviour would not be observed within a formulation



811 based on standard Fick’s law, at least with our model as is.

812 Finally, as we mentioned before (see Remark [3](#)), for completeness in our discussion, we compare  
813 the results corresponding to the adoption of  $\mathcal{N}(\alpha)$  versus those obtained with  $\hat{\mathcal{N}}(\alpha)$ . As shown  
814 in Fig. [6](#), top left panel, when the normalisation factor is  $\hat{\mathcal{N}}(\alpha)$ , we observe, for  $\alpha \rightarrow 0^+$ , a less  
815 pronounced decrease of the nutrients’ mass fraction. This is compatible with the fact that, even for  
816 very small values of  $\alpha$ , there is an incoming mass flux of nutrients through the domain’s boundaries  
817 that reestablishes the nutrients eaten by the cells. This effect, in turn, tends to disappear when  
818 the normalisation factor  $\mathcal{N}(\alpha)$  is employed since, in that case, the mass flux tends to zero in the  
819 limit  $\alpha \rightarrow 0^+$ . Coherently with this observation, we also notice a markedly different behaviour of  
820 the growth parameter (see Fig. [6](#), top right panel). Indeed, since the flux of nutrients obtained  
821 for  $\hat{\mathcal{N}}(\alpha)$  does not vanish for  $\alpha \rightarrow 0^+$ , and a greater amount of nutrients remains available even  
822 at time  $t = 20$  d, growth can still occur, as is testified by the dotted line marked with “+”.  
823 Similar comments pertain also to the description of the displacement (see Fig. [6](#), bottom left  
824 panel). Indeed, since growth remains active also for small values of  $\alpha$ , the displacement also tends  
825 to persist even at  $t = 20$  d, and remains relatively large in the neighbourhood of the domain’s  
826 boundaries, where the availability of nutrients is the highest (because of the Dirichlet condition  
827 assigned to the nutrients’ mass fraction) and growth is present. These differences notwithstanding,  
828 it should be emphasised that the qualitative behaviour of the curves describing the nutrients’ mass  
829 fraction and the growth parameter is the same for both choices of the normalisation factor. On the  
830 contrary, the behaviour of the pressure (see Fig. [6](#), bottom right panel) is *both* qualitatively *and*  
831 quantitatively different for  $\alpha = 0.1$ . In fact, the use of  $\hat{\mathcal{N}}(\alpha)$  nullifies the effect visible at  $t = 20$  d,  
832 for  $\alpha = 0.1$  and normalisation factor  $\mathcal{N}(\alpha)$ , which consisted in the sign change of the pressure.  
833 Hence, employing  $\hat{\mathcal{N}}(\alpha)$  leaves the pressure negative, thereby triggering no inversion in the flow of  
834 the interstitial fluid, which continues to flow from the exterior of the tumour into it.

## 835 9 Conclusions

836 In this work, we study the influence of a given type of non-local diffusion of nutrients on the growth  
837 of an avascular tumour. For this purpose, we generalise Fick’s law of diffusion by introducing a  
838 non-local constitutive relationship for the mass flux vector that, after some considerations, can be  
839 identified with a fractional derivative of the nutrients’ mass fraction. We call attention to the fact  
840 that, since we are dealing with growth, we need to describe how the non-locality of the prescribed  
841 constitutive law evolves with the deformation and the growth-induced inelastic distortions that  
842 accompany the evolution of the system under study. This consideration implies that the non-  
843 locality of the presumed constitutive response should be subordinate to the motion  $\chi$  (see Equation  
844 [\(22b\)](#)) and, thus, that it cannot depend explicitly on the difference  $X - \tilde{X}$  between the reference  
845 placements of the material points embedded in  $X$  and  $\tilde{X}$ . Furthermore, we note that, as prescribed  
846 by Equation [\(25\)](#), the non-local character of the mass flux vector also depends on the structural  
847 changes of the tumour through the determinant of  $\mathbf{F}_\gamma$ . To the best of our understanding, the above  
848 considerations imply substantial differences between our work and other papers on the subject  
849 found in the scientific literature. Moreover, we suggest a formulation of non-local diffusion on  
850 manifolds (see Appendix A1).

851 To investigate the influence of the non-local diffusion of the nutrients on the tumour evolution,  
852 we focused on a benchmark problem that allows, due to the enforced symmetries, the reduction

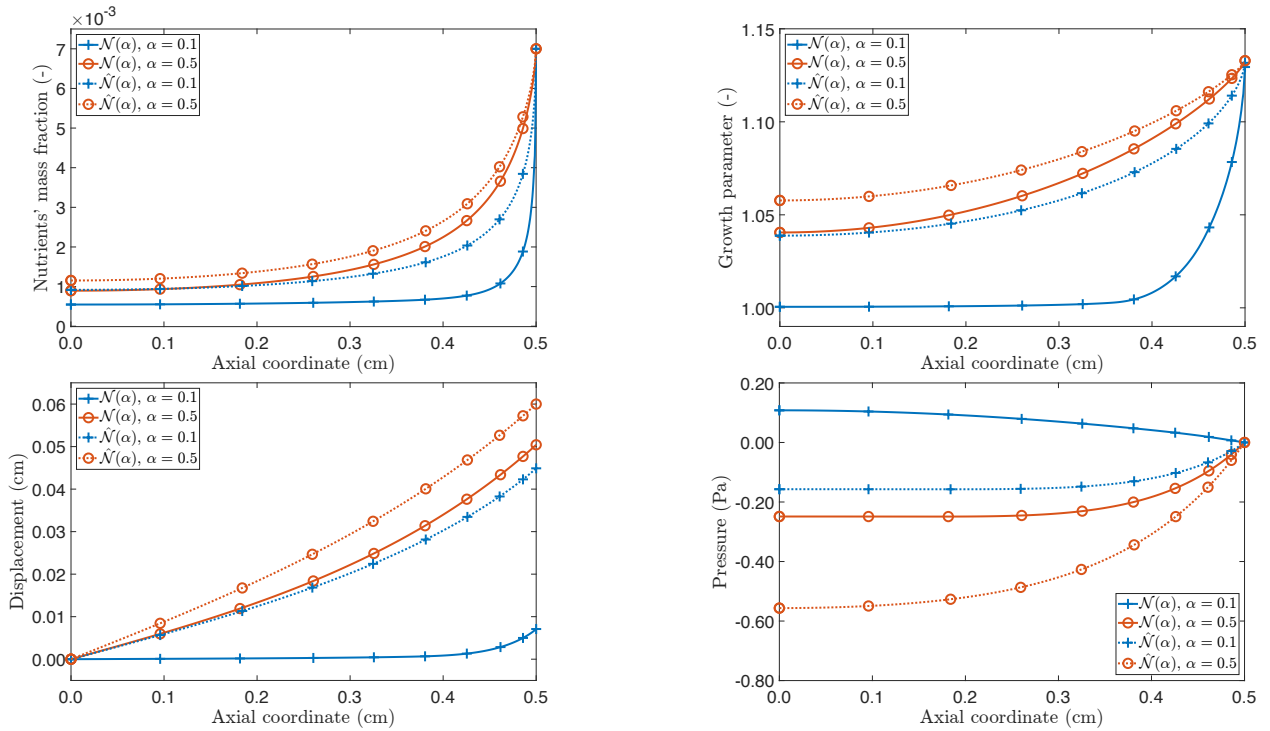


Figure 6: Comparison of the spatial profiles of  $\mathbf{c}_a(Z, t)$  (top left),  $\gamma(Z, t)$  (top right),  $u(Z, t)$  (bottom left) and  $\mathbf{p}(Z, t)$  (bottom right) for the approaches involving  $\mathcal{N}(\alpha)$  (solid line) and  $\hat{\mathcal{N}}(\alpha)$  (dotted line). In the plots different values of  $\alpha$  are used and time is fixed to  $t = 20$  d.

853 of the original three-dimensional framework to a one-dimensional problem. This has an important  
 854 impact on the selection of the non-locality function,  $\hat{f}_\alpha$ , which has to be able to capture how the  
 855 geometrical symmetries of the problem affect the description of the non-locality. Particularly, in  
 856 our analysis, we re-obtained the definition of one-dimensional fractional mass flux proposed in other  
 857 works [89, 35].

858 In our work, the numerical solution of the set of equations defining the mathematical model  
 859 is found by employing the FE method, which has been adapted for the solution of the fractional  
 860 diffusion equation (26c). In particular, the obtained numerical results show that the non-local  
 861 character of the nutrients' evolution has a considerable repercussion on the growth of the hypo-  
 862 theoretical tumour under study. Specifically, by varying the parameter  $\alpha \in ]0, 1[$ , the model is capable,  
 863 in the limit cases, of generating situations of no diffusion or of restoring Fick's law. This conclu-  
 864 sion evidences the relevance of embracing a fractional framework in our model, since it permits to  
 865 "control", through the parameter  $\alpha$ , the way in which the tumour grows. Finally, we discussed a  
 866 possible way for defining another normalisation factor, termed  $\hat{\mathcal{N}}(\alpha)$ , involved in the definition of  
 867 the mass flux vector, and we provided a comparison between the two approaches.

868 Certainly, our model can be further generalised and, in the following, we discuss some important  
 869 issues that should be accounted for in forthcoming works. A first issue arises from the fact that,  
 870 once the dimensionality and the symmetries of the problem at hand are specified, Equation (16)  
 871 must be adapted accordingly. This implies that the non-locality function and the normalisation

872 factors should be conceived in a symmetry- and dimensional-dependent fashion<sup>2</sup>. To find such  
873 relations is part of our ongoing research. Additionally, in our model, the information on the  
874 microscopic structure of the tumour is not explicitly taken into account and, thus, its contribution  
875 is neglected. As pointed out in the Introduction, the multi-scale and heterogeneous character of the  
876 environment in which diffusion takes place is one of the main factors influencing the occurrence of  
877 non-Fickian diffusion. Therefore, the adoption of mathematical techniques, such as the Asymptotic  
878 Homogenisation Method [29], could be capable of incorporating these features into a framework of  
879 tissue growth [96] and non-local diffusion.

880 We further remark that an aspect that is not contemplated in the current formulation of the  
881 model is that the chemical agents should be both in the fluid phase and in the solid phase, and not  
882 only in the fluid phase. One of the main drawbacks of this phenomenological consideration is that it  
883 is not possible to link the mass sources to the chemical potentials of the nutrients, nor is it possible  
884 to establish a sound and comprehensive thermodynamic framework accounting for interphase mass  
885 transfers as non-equilibrium processes. This implies that no information, or only a limited amount  
886 of information, can be extracted from the study of the dissipation inequality of the system (and this  
887 is not directly due to the fact that growth necessitates the consideration of processes, of cellular or  
888 molecular type, that could not be accounted for in the model). Therefore, under the circumstances  
889 of the present model, it is not possible to obtain Equation (16) from the study of the dissipation  
890 inequality, as it would be the case in the classical procedure that leads to Fick's law. In this respect,  
891 one of the technical difficulties that arise in our work is that we cannot invert the balance of linear  
892 momentum associated with the chemical agents, since the inversion of fractional operators is not  
893 always permitted. One possible solution, that seems to be thermodynamically acceptable, is to  
894 adopt a procedure similar to the one depicted in [58], that is, to consider the part of the dissipation  
895 inequality that is of interest for us, to put it in weak form and to express the flux in terms of a  
896 non-local constitutive law depending on the gradient of the chemical potential.

897 Finally, we would like to mention that in recent years Fractional Calculus has demonstrated to  
898 be an effective mathematical tool in the description of several phenomena. However, there is still  
899 an urgency in incorporating this notion in mathematical models that go beyond the classical ones.

## 900 Acknowledgement

901 The Authors acknowledge the *Dipartimento di Scienze Matematiche* (DISMA) "G.L. Lagrange" of  
902 the *Politecnico di Torino*, and that the present research has been partially supported by MIUR  
903 grant "Dipartimenti di Eccellenza 2018–2022" ('Departments of Excellence 2018–2022'), project  
904 no. E11G18000350001. The Authors warmly thank Prof. Dušan Zorica for his invaluable help, for  
905 providing essential references and for the many suggestions that he has given us for this work.

## 906 Authors contribution

907 All Authors have equally contributed to this work.

---

<sup>2</sup>Similar problems are subject of investigations conducted by our group in conjunction with our colleague Prof. Dušan Zorica (Mathematical Institute, Serbian Academy of Arts and Sciences, Serbia) and started, from our side, during his visit at the *Politecnico di Torino* (Italy) in January 2020.

## 908 Conflict of Interests

909 The Authors declare that they have no conflict of interests.

## 910 A A1 Some aspects of non-locality on manifolds

911 In the following, we propose a possible way for the formulation of non-local diffusion on manifolds.  
 912 For this purpose, let us recall that the fractional mass flux vector  $\mathbf{y}_\alpha$  is defined through the duality  
 913 product

$$\langle \mathbf{y}_\alpha, \text{grad } \check{c} \rangle := -\varrho_f \int_{\mathcal{B}_t} \left\{ \int_{\mathcal{B}_t} [\text{grad } \check{c}(x)] \mathbf{d}_\alpha(x, \tilde{x}, t) [\text{grad } c_a(\tilde{x}, t)] \text{d}v(\tilde{x}) \right\} \text{d}v(x), \quad (65a)$$

$$\mathbf{d}_\alpha(x, \tilde{x}, t) := \mathfrak{f}_\alpha(x, \tilde{x}) \mathfrak{d}_\alpha(x, \tilde{x}, t), \quad (65b)$$

914 where the non-locality function is given by the following relationship

$$\mathfrak{f}_\alpha(x, \tilde{x}) := \mathfrak{f}_\alpha^{(0)}(x_0, \mathcal{T}_x^{x_0}(\tilde{x})). \quad (66)$$

915 In Equation (66), the notation  $\mathcal{T}_x^{x_0} := \exp_{x_0} \circ (\mathcal{P}_{x_0}^x)^{-1} \circ \exp_x^{-1}$  is used, and the following operators  
 916 are introduced:

- 917 • Let  $T_{x,\delta}\mathcal{B}_t$  be the subset of the tangent space  $T_x\mathcal{B}_t$  defined by

$$T_{x,\delta}\mathcal{B}_t := \{\mathbf{v}_x \in T_x\mathcal{B}_t \mid \langle \mathbf{v}_x, \mathbf{v}_x \rangle_{\mathbf{g}} \leq \delta, \text{ with } \delta > 0\}, \quad (67)$$

918 and let  $\mathcal{U}_t(x, \delta) := \{\tilde{x} \in \mathcal{B}_t \mid \text{dist}_{\mathcal{B}_t}(x, \tilde{x}) \leq \delta\}$  be a closed neighbourhood of  $x$  having radius  
 919  $\delta$ , with  $\text{dist}_{\mathcal{B}_t} : \mathcal{B}_t \times \mathcal{B}_t \rightarrow \mathbb{R}_0^+$  denoting the *distance function*<sup>3</sup> on  $\mathcal{B}_t$  [106]. The operator

$$\exp_x : T_{x,\delta}\mathcal{B}_t \rightarrow \mathcal{U}_t(x, \delta), \quad (68)$$

920 referred to as *exponential map*, is injective and associates each element of  $T_{x,\delta}\mathcal{B}_t$  with the  
 921 point  $\tilde{x} = \exp_x(\mathbf{v}_x) \in \mathcal{U}_t(x, \delta)$ , which is the projection of  $\mathbf{v}_x$  onto  $\mathcal{U}_t(x, \delta)$ . Note that the  
 922 result of this operation generalises the concept of translation to the case of a manifold. To  
 923 construct  $\exp_x(\mathbf{v}_x)$ , we take  $\mathbf{v}_x \in T_{x,\delta}\mathcal{B}_t$  and consider the unique solution to the geodesic  
 924 equation (see e.g. [79]), parameterised by  $\eta : [0, 1] \rightarrow \mathcal{U}_t(x, \delta)$ , and in harmony with the  
 925 ‘‘initial’’ conditions  $\eta(0) = x$  and  $\eta'(0) = \mathbf{v}_x$ . Then, we identify  $\exp_x(\mathbf{v}_x)$  with  $\eta(1)$ , i.e.,  
 926  $\exp_x(\mathbf{v}_x) = \eta(1) \equiv \tilde{x}$ .

927 By construction, the exponential map is invertible and its inverse, i.e.,  $\exp_x^{-1} : \mathcal{U}_t(x, \delta) \rightarrow$   
 928  $T_{x,\delta}\mathcal{B}_t$ , returns a unique tangent vector of  $T_{x,\delta}\mathcal{B}_t$  for each point of  $\mathcal{U}_t(x, \delta)$ . Therefore, by  
 929 taking  $\tilde{x} \in \mathcal{U}_t(x, \delta)$ , with  $\tilde{x} = \eta(1)$ , it holds that  $\exp_x^{-1}(\eta(1)) = \eta'(0)$ .

930 <sup>3</sup>Given the geodesic from  $x$  to  $\tilde{x}$ , and denoting by  $\eta : [0, 1] \rightarrow \mathcal{B}_t$  its parameterisation, so that  $x = \eta(0)$   
 and  $\tilde{x} = \eta(1)$ , we set  $\text{dist}_{\mathcal{B}_t}(x, \tilde{x}) := \int_0^1 \|\eta'(\sigma)\| \text{d}\sigma$ .

931 • Let us consider two points of the manifold, e.g.  $x_0, x \in \mathcal{B}_t$ , and let  $\zeta : [0, s] \rightarrow \mathcal{B}_t$ , with  
 932  $\zeta(0) = x_0$  and  $\zeta(s) = x$ , be the parameterisation of the geodesic connecting  $x_0$  to  $x$ . Moreover,  
 933 let us take the sets of tangent vectors  $T_{x_0, \delta} \mathcal{B}_t$  and  $T_{x, \delta} \mathcal{B}_t$ , with  $\delta > 0$ . Then, to transport  
 934 parallelly the elements of  $T_{x_0, \delta} \mathcal{B}_t$  into  $T_{x, \delta} \mathcal{B}_t$  along the geodesic parameterised by  $\zeta$ , we define  
 935 the shifter operator

$$\mathcal{P}_{x_0}^x : T_{x_0, \delta} \mathcal{B}_t \rightarrow T_{x, \delta} \mathcal{B}_t, \quad \mathbf{v}_{x_0} \mapsto \mathcal{P}_{x_0}^x \mathbf{v}_{x_0} = \mathbf{v}_x. \quad (69)$$

936 Clearly,  $\mathcal{P}_{x_0}^x$  is invertible and its inverse reads  $(\mathcal{P}_{x_0}^x)^{-1} = \mathcal{P}_{x_0}^{x_0} : T_{x, \delta} \mathcal{B}_t \rightarrow T_{x_0, \delta} \mathcal{B}_t$ . In addition,  
 937  $\mathcal{P}_{x_0}^{x_0}$  is the identity operator from  $T_{x_0, \delta} \mathcal{B}_t$  into itself.

938

939 • To represent  $\mathfrak{f}_\alpha(x, \tilde{x})$  properly, we explain in detail our understanding of the procedure  
 940 sketched in [106]. For this purpose, we start recalling that  $\mathfrak{f}_\alpha(x, \tilde{x})$  measures how, at time  $t$ ,  
 941 the value of  $\text{grad} c_a(\tilde{x}, t)$  is “felt” at  $x$ , for all pairs of points  $x, \tilde{x} \in \mathcal{B}_t$ , such that  $\tilde{x} \in \mathcal{U}_t(x, \delta)$ ,  
 942 with  $\delta > 0$ . This influence has to be described in a way respectful of the geometry of the  
 943 manifold, which can be achieved as follows. Given  $\mathfrak{f}_\alpha(x, \tilde{x})$ , we select arbitrarily a point  
 944  $x_0 \in \mathcal{B}_t$  and we introduce an auxiliary function  $\mathfrak{f}_\alpha^{(0)}(x_0, \cdot) : \mathcal{U}_t(x_0, \delta) \rightarrow \mathbb{R}$ , such that, for an  
 945 appropriate  $\tilde{x}_0 \in \mathcal{U}_t(x_0, \delta)$ ,  $\mathfrak{f}_\alpha^{(0)}(x_0, \tilde{x}_0) = \mathfrak{f}_\alpha(x, \tilde{x})$ . In order for  $\tilde{x}_0$  to be “appropriate”, it has  
 946 to depend on  $x$  and  $\tilde{x}$  (and on  $x_0$ ). This can be obtained by calling for the operator

$$\mathcal{T}_x^{x_0} := \exp_{x_0} \circ (\mathcal{P}_{x_0}^x)^{-1} \circ \exp_x^{-1} : \mathcal{U}_t(x, \delta) \rightarrow \mathcal{U}_t(x_0, \delta). \quad (70)$$

947 As anticipated above, for each  $\tilde{x} \in \mathcal{U}_t(x, \delta)$ ,  $\exp_x^{-1}$  returns a vector  $\mathbf{v}_x$ , such that  $\|\mathbf{v}_x\| \leq \delta$ .  
 948 Then,  $(\mathcal{P}_{x_0}^x)^{-1}$  transports  $\mathbf{v}_x$  parallelly to  $x_0$ , so that  $(\mathcal{P}_{x_0}^x)^{-1} \mathbf{v}_x = \mathbf{v}_{x_0}$ . Finally, the operator  
 949  $\exp_{x_0}$  maps  $\mathbf{v}_{x_0}$  into  $\tilde{x}_0 = \exp_{x_0}(\mathbf{v}_{x_0}) \in \mathcal{U}_t(x_0, \delta)$ . Therefore, it holds that  $\tilde{x}_0 = \mathcal{T}_x^{x_0}(\tilde{x})$ ,  
 950 thereby explaining how  $\tilde{x}_0$  depends on  $x$  and  $\tilde{x}$ , for a given  $x_0$ . More specifically, the action  
 951 of  $\mathcal{T}_x^{x_0}$  on  $\tilde{x}$  permits to find the only  $\tilde{x}_0$  such that Equation (66) becomes

$$\mathfrak{f}_\alpha(x, \tilde{x}) = \mathfrak{f}_\alpha^{(0)}(x_0, \mathcal{T}_x^{x_0}(\tilde{x})) = \mathfrak{f}_\alpha^{(0)}(x_0, \tilde{x}_0), \quad (71)$$

952 where the composition  $\mathfrak{f}_\alpha(x, \cdot) = \mathfrak{f}_\alpha^{(0)}(x_0, \cdot) \circ \mathcal{T}_x^{x_0} : \mathcal{U}_t(x, \delta) \rightarrow \mathbb{R}$  is implied. The essence of  
 953 this result is that the information on the non-locality of a given phenomenon between  $x$  and  
 954  $\tilde{x}$ , encompassed by  $\mathfrak{f}_\alpha(x, \tilde{x})$ , is “transported” to the pair of points  $x_0$  and  $\tilde{x}_0$  (see Fig. 7).

955 To conclude, we notice that, in an affine space or, more generally, in a flat subset of an affine  
 956 space, the procedure outlined above boils down to the determination of the unique point  $\tilde{x}_0$   
 957 such that  $\mathbf{v}_{x_0} = \tilde{x}_0 - x_0$  is equipollent to  $\mathbf{v}_x = \tilde{x} - x$ , for given  $x_0, x$  and  $\tilde{x}$ . Indeed, within  
 958 this framework,  $\mathcal{T}_x^{x_0}$  operates in such a way that  $\mathbf{v}_{x_0} = \mathcal{T}_x^{x_0}(\tilde{x}) - x_0 = \tilde{x}_0 - x_0$  is parallel to  $\mathbf{v}_x$   
 959 (because  $\mathbf{v}_x$  is transported parallelly along the geodesic —now, a straight line— connecting  $x$   
 960 with  $x_0$ ) and  $\|\mathbf{v}_{x_0}\| \equiv \|\tilde{x}_0 - x_0\| = \|\tilde{x} - x\| \equiv \|\mathbf{v}_x\|$ . Moreover,  $\mathfrak{f}_\alpha(x, \tilde{x})$  and  $\mathfrak{f}_\alpha^{(0)}(x_0, \tilde{x}_0)$  can be  
 961 rephrased as  $\mathfrak{f}_\alpha(x, \tilde{x}) = \hat{\mathfrak{f}}_\alpha(x - \tilde{x})$  and  $\mathfrak{f}_\alpha^{(0)}(x_0, \tilde{x}_0) = \hat{\mathfrak{f}}_\alpha(x_0 - \tilde{x}_0)$ , respectively, and Equation  
 962 (66), or Equation (71), is trivially satisfied. In this respect, we say that Equation (66) adapts  
 963 the meaning of convolution from the case of an affine space to the case of a manifold (see  
 964 Fig. 8).

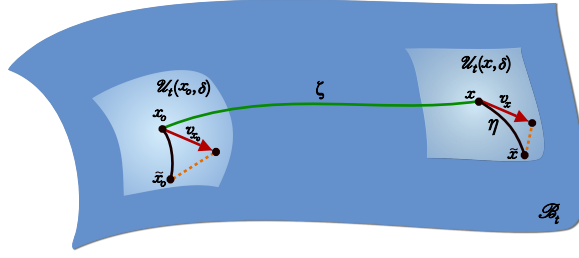


Figure 7: The convolution on manifolds is defined by transporting  $f_\alpha(x, \cdot) : \mathcal{U}_t(x, \delta) \rightarrow \mathbb{R}$  to every point of  $\mathcal{B}_t$ , while taking into account the manifold geometry. Thus, given a point  $\tilde{x} = \eta(1) \in \mathcal{U}_t(x, \delta)$ , the operation  $\exp_x^{-1}(\tilde{x})$  returns the vector  $\mathbf{v}_x = \eta'(0)$ , which is parallelly transported to  $\mathbf{v}_{x_0}$  through a geodesic  $\zeta : [0, s] \rightarrow \mathcal{B}_t$  connecting  $x = \zeta(s)$  and  $x_0 = \zeta(0)$ , and the operation  $\exp_{x_0}(\mathbf{v}_{x_0})$  returns the point  $\tilde{x}_0 \in \mathcal{U}_t(x_0, \delta)$ . In this way,  $f_\alpha(x, \cdot)$  is transported from  $\mathcal{U}_t(x, \delta)$  to  $\mathcal{U}_t(x_0, \delta)$ .

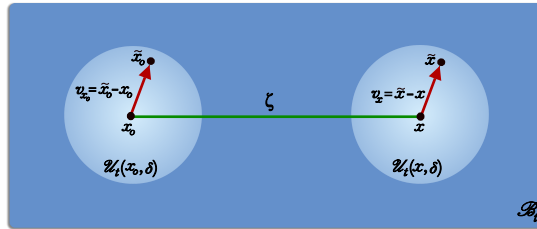


Figure 8: In a flat subset of an affine space  $\mathbf{v}_{x_0} = \tilde{x}_0 - x_0$  is equipollent to  $\mathbf{v}_x = \tilde{x} - x$ . Therefore,  $f_\alpha(x, \tilde{x})$  and  $f_\alpha^{(0)}(x_0, \tilde{x}_0)$  can be rephrased as  $f_\alpha(x, \tilde{x}) = \hat{f}_\alpha(x - \tilde{x})$  and  $f_\alpha^{(0)}(x_0, \tilde{x}_0) = \hat{f}_\alpha^{(0)}(x_0 - \tilde{x}_0)$ .

## 965 References

- 966 [1] Fayçal Ben Adda. La différentiabilité dans le calcul fractionnaire. *Comptes Rendus de*  
967 *l'Académie des Sciences - Series I - Mathematics*, 326(7):787–791, apr 1998.
- 968 [2] Elias C Aifantis and James B Serrin. The mechanical theory of fluid interfaces and maxwell's  
969 rule. *Journal of Colloid and Interface Science*, 96(2):517–529, dec 1983.
- 970 [3] Gioacchino Alotta, Mario Di Paola, Francesco Paolo Pinnola, and Massimiliano Zingales. A  
971 fractional nonlocal approach to nonlinear blood flow in small-lumen arterial vessels. *Mecca-*  
972 *nica*, 55(4):891–906, mar 2020.
- 973 [4] D. Ambrosi, G.A. Ateshian, E.M. Arruda, S.C. Cowin, J. Dumais, A. Goriely, G.A. Holzapfel,  
974 J.D. Humphrey, R. Kemkemer, E. Kuhl, J.E. Olberding, L.A. Taber, and K. Garikipati.  
975 Perspectives on biological growth and remodeling. *Journal of the Mechanics and Physics of*  
976 *Solids*, 59(4):863–883, apr 2011.
- 977 [5] D. Ambrosi and F. Mollica. On the mechanics of a growing tumor. *International Journal of*  
978 *Engineering Science*, 40(12):1297–1316, jul 2002.

- 979 [6] D. Ambrosi and L. Preziosi. On the closure of mass balance models for tumor growth.  
980 *Mathematical Models and Methods in Applied Sciences*, 12(05):737–754, may 2002.
- 981 [7] D. Ambrosi, L. Preziosi, and G. Vitale. The insight of mixtures theory for growth and  
982 remodeling. *Z. Angew. Math. Phys.*, 61:177–191, 2010.
- 983 [8] R. P. Araujo and D. L. McElwain. A history of the study of solid tumour growth: the  
984 contribution of mathematical modelling. *Bulletin of Mathematical Biology*, may 2004.
- 985 [9] T. M. Atanacković, S. Pilipović, B. Stanković, and D. Zorica. *Fractional Calculus with*  
986 *Applications in Mechanics: Vibrations and Diffusion Processes*. ISTE Ltd., 2014.
- 987 [10] T M Atanackovic, S Pilipovic, and D Zorica. A diffusion wave equation with two frac-  
988 tional derivatives of different order. *Journal of Physics A: Mathematical and Theoretical*,  
989 40(20):5319–5333, apr 2007.
- 990 [11] T. M. Atanackovic and B. Stankovic. Generalized wave equation in nonlocal elasticity. *Acta*  
991 *Mechanica*, 208(1-2):1–10, nov 2008.
- 992 [12] Teodor M. Atanacković, S. Pilipović, B. Stanković, and D. Zorica. *Fractional Calculus with*  
993 *Applications in Mechanics: Wave Propagation, Impact and Variational Principles*. ISTE  
994 Ltd., 2014.
- 995 [13] G.A. Ateshian and J.A. Weiss. Anisotropic hydraulic permeability under finite deformation.  
996 *J. Biomech. Engng.*, 132:111004–1–111004–7, 2010.
- 997 [14] N. Bellomo and L. Preziosi. Modelling and mathematical problems related to tumor evolution  
998 and its interaction with the immune system. *Mathematical and Computer Modelling*, 32(3-  
999 4):413–452, aug 2000.
- 1000 [15] L.S. Bennethum, M.A. Murad, and J.H. Cushman. Macroscale thermodynamics and the  
1001 chemical potential for swelling porous media. *Transport in Porous Media*, 39(2):187–225,  
1002 2000.
- 1003 [16] Haim Brezis. *Functional Analysis, Sobolev Spaces and Partial Differential Equations*. Springer  
1004 New York, 2010.
- 1005 [17] Michael M. Bronstein, Joan Bruna, Yann LeCun, Arthur Szlam, and Pierre Vandergheynst.  
1006 Geometric deep learning: Going beyond euclidean data. *IEEE Signal Processing Magazine*,  
1007 34(4):18–42, jul 2017.
- 1008 [18] Alfonso Bueno-Orovio, David Kay, Vicente Grau, Blanca Rodriguez, and Kevin Burrage.  
1009 Fractional diffusion models of cardiac electrical propagation: role of structural heterogeneity  
1010 in dispersion of repolarization. *Journal of The Royal Society Interface*, 11(97):20140352, aug  
1011 2014.
- 1012 [19] H. Byrne and L. Preziosi. Modelling solid tumour growth using the theory of mixtures.  
1013 *Mathematical Medicine and Biology*, 20(4):341–366, dec 2003.



- 1014 [20] H.M. Byrne and M.A. Chaplain. Growth of nonnecrotic tumors in the presence and absence  
1015 of inhibitors. *Mathematical biosciences*, 130:151–181, December 1995.
- 1016 [21] Silvia Capuani, Marco Palombo, Andrea Gabrielli, Augusto Orlandi, Bruno Maraviglia, and  
1017 Francesco S. Pastore. Spatio-temporal anomalous diffusion imaging: results in controlled  
1018 phantoms and in excised human meningiomas. *Magnetic Resonance Imaging*, 31(3):359–365,  
1019 apr 2013.
- 1020 [22] A. Carpinteri, P. Cornetti, and A. Saporà. A fractional calculus approach to nonlocal elas-  
1021 ticity. *The European Physical Journal Special Topics*, 193(1):193–204, mar 2011.
- 1022 [23] J.J. Casciari, S.V. Sotirchos, and R.M. Sutherland. Mathematical modelling of microenviron-  
1023 ment and growth in EMT6/ro multicellular tumour spheroids. *Cell Proliferation*, 25(1):1–22,  
1024 jan 1992.
- 1025 [24] Joseph J. Casciari, Stratis V. Sotirchos, and Robert M. Sutherland. Variations in tumor  
1026 cell growth rates and metabolism with oxygen concentration, glucose concentration, and  
1027 extracellular pH. *Journal of Cellular Physiology*, 151(2):386–394, may 1992.
- 1028 [25] M.A.J. Chaplain, L. Graziano, and L. Preziosi. Mathematical modelling of the loss of tissue  
1029 compression responsiveness and its role in solid tumour development. *Mathematical Medicine  
1030 and Biology: A Journal of the IMA*, 23(3):197–229, sep 2006.
- 1031 [26] A.S. Chaves. A fractional diffusion equation to describe lévy flights. *Physics Letters A*,  
1032 239(1-2):13–16, feb 1998.
- 1033 [27] V. Ciancio, M. Dolfín, M. Francaviglia, and S. Preston. Uniform materials and the multi-  
1034 plicative decomposition of the deformation gradient in finite elasto-plasticity. *J. Non-Equilib.  
1035 Thermodyn.*, 33(3):199–234, 2008.
- 1036 [28] P. Ciarletta, M. Destrade, and A. L. Gower. On residual stresses and homeostasis: an elastic  
1037 theory of functional adaptation in living matter. *Scientific Reports*, 6(1), apr 2016.
- 1038 [29] D Cioranescu. *An introduction to homogenization*. Oxford University Press, 1999.
- 1039 [30] S. Cleja-Tigoiu and G. A. Maugin. Eshelby’s stress tensors in finite elastoplasticity. *Acta  
1040 Mechanica*, 139(1-4):231–249, mar 2000.
- 1041 [31] Helena L.E. Coker, Matthew R. Cheetham, Daniel R. Kattnig, Yong J. Wang, Sergi Garcia-  
1042 Manyes, and Mark I. Wallace. Controlling anomalous diffusion in lipid membranes. *Biophys-  
1043 ical Journal*, 116(6):1085–1094, mar 2019.
- 1044 [32] S. C. Cowin and G. A. Holzapfel. On the modeling of growth and adaptation. In Holzapfel G.  
1045 A. and Odgen R. W., editors, *Mechanics of Biological Tissue*, pages 29–46. Springer-Verlag,  
1046 2006.
- 1047 [33] E. Crevacore, S. Di Stefano, and A. Grillo. Coupling among deformation, fluid flow, struc-  
1048 tural reorganisation and fibre reorientation in fibre-reinforced, transversely isotropic biological  
1049 tissues. *International Journal of Nonlinear Mechanics*, In press, 2018.

- 1050 [34] Y. Danyuo, C. J. Ani, A. A. Salifu, J. D. Obayemi, S. Dozie-Nwachukwu, V. O. Obanawu,  
1051 U. M. Akpan, O. S. Odusanya, M. Abade-Abugre, F. McBagonluri, and W. O. Soboyejo.  
1052 Anomalous release kinetics of prodigiosin from poly-n-isopropyl-acrylamid based hydrogels  
1053 for the treatment of triple negative breast cancer. *Scientific Reports*, 9(1), mar 2019.
- 1054 [35] D. del Castillo-Negrete. Fractional diffusion models of nonlocal transport. *Physics of Plasmas*,  
1055 13(8):082308, aug 2006.
- 1056 [36] Zhi-Qiang Deng, Vijay P. Singh, and Lars Bengtsson. Numerical solution of fractional  
1057 advection-dispersion equation. *Journal of Hydraulic Engineering*, 130(5):422–431, may 2004.
- 1058 [37] Mario Di Paola and Massimiliano Zingales. Long-range cohesive interactions of non-local  
1059 continuum faced by fractional calculus. *International Journal of Solids and Structures*,  
1060 45(21):5642–5659, oct 2008.
- 1061 [38] Mario Di Paola and Massimiliano Zingales. Fractional differential calculus for 3d mechanically  
1062 based non-local elasticity. *International Journal for Multiscale Computational Engineering*,  
1063 9(5):579–597, 2011.
- 1064 [39] A. DiCarlo and S. Quiligotti. Growth and balance. *Mechanics Research Communications*,  
1065 29(6):449–456, nov 2002.
- 1066 [40] Nader Engheta. Fractional curl operator in electromagnetics. *Microwave and Optical Tech-*  
1067 *nology Letters*, 17(2):86–91, feb 1998.
- 1068 [41] M. Epstein. Self-driven continuous dislocations and growth. In Maugin G.A. Steinmann P.,  
1069 editor, *Mechanics of Material Forces. Advances in Mechanics and Mathematics*, volume 11,  
1070 pages 129–139. Springer, Boston, MA, 2005.
- 1071 [42] M. Epstein and G.A. Maugin. Thermomechanics of volumetric growth in uniform bodies.  
1072 *International Journal of Plasticity*, 16(7-8):951–978, jun 2000.
- 1073 [43] A. Cemal Eringen. Linear theory of nonlocal elasticity and dispersion of plane waves. *Inter-*  
1074 *national Journal of Engineering Science*, 10(5):425–435, may 1972.
- 1075 [44] Gissell Estrada-Rodriguez, Heiko Gimperlein, Kevin J. Painter, and Jakub Stoczek. Space-  
1076 time fractional diffusion in cell movement models with delay. *Mathematical Models and*  
1077 *Methods in Applied Sciences*, 29(01):65–88, jan 2019.
- 1078 [45] N. Filipovitch, K. M. Hill, A. Longjas, and V. R. Voller. Infiltration experiments demon-  
1079 strate an explicit connection between heterogeneity and anomalous diffusion behavior. *Water*  
1080 *Resources Research*, 52(7):5167–5178, jul 2016.
- 1081 [46] G. Forgacs, R.A. Foty, Y. Shafir, and M.S. Steinberg. Viscoelastic properties of living  
1082 embryonic tissues: a quantitative study. *Biophysical Journal*, 74:2227–2234, 1998.
- 1083 [47] P. Fuschi, A. A. Pisano, and D. De Domenico. Plane stress problems in nonlocal elasticity:  
1084 finite element solutions with a strain-difference-based formulation. *Journal of Mathematical*  
1085 *Analysis and Applications*, 431(2):714–736, nov 2015.

- 1086 [48] Naama Gal and Daphne Weihs. Experimental evidence of strong anomalous diffusion in living  
1087 cells. *Physical Review E*, 81(2), feb 2010.
- 1088 [49] Heiko Gimperlein and Jakub Stoczek. Space–time adaptive finite elements for nonlocal  
1089 parabolic variational inequalities. *Computer Methods in Applied Mechanics and Engineering*,  
1090 352:137–171, aug 2019.
- 1091 [50] C. Giverso and L. Preziosi. Modelling the compression and reorganization of cell aggregates.  
1092 *Mathematical Medicine and Biology*, 29:181–204, 2012.
- 1093 [51] C. Giverso, M. Scianna, and A. Grillo. Growing avascular tumours as elasto-plastic bodies  
1094 by the theory of evolving natural configurations. *Mech. Res. Commun.*, 68:31–39, 2015.
- 1095 [52] A. Goriely. *The Mathematics and Mechanics of Biological Growth*. Springer New York, 2016.
- 1096 [53] A. Grillo, M. Carfagna, and S. Federico. Non-Darcian flow in fibre-reinforced biological  
1097 tissues. *Meccanica*, 52:3299–3320, 2017.
- 1098 [54] A. Grillo, S. Federico, and G. Wittum. Growth, mass transfer, and remodeling in fiber-  
1099 reinforced, multi-constituent materials. *Int. J. Nonlinear Mech.*, 47:388–401, 2012.
- 1100 [55] A. Grillo, R. Prohl, and G. Wittum. A poroplastic model of structural reorganisation in  
1101 porous media of biomechanical interest. *Continuum Mech. Therm.*, 28:579–601, 2016.
- 1102 [56] Alfio Grillo, Salvatore Di Stefano, Ariel Ramírez-Torres, and Michele Loverre. A study of  
1103 growth and remodeling in isotropic tissues, based on the anand-aslan-chester theory of strain-  
1104 gradient plasticity. *GAMM-Mitteilungen*, 42(4), may 2019.
- 1105 [57] Morton E. Gurtin. On the plasticity of single crystals: free energy, microforces, plastic-strain  
1106 gradients. *Journal of the Mechanics and Physics of Solids*, 48(5):989–1036, may 2000.
- 1107 [58] Klaus Hackl and Franz Dieter Fischer. On the relation between the principle of maximum  
1108 dissipation and inelastic evolution given by dissipation potentials. *Proceedings of the Royal  
1109 Society A: Mathematical, Physical and Engineering Sciences*, 464(2089):117–132, oct 2007.
- 1110 [59] Kotaybah Hashlamoun, Ziad Abusara, Ariel Ramírez-Torres, Alfio Grillo, Walter Herzog,  
1111 and Salvatore Federico. Fluorescence recovery after photobleaching: direct measurement of  
1112 diffusion anisotropy. *Biomechanics and Modeling in Mechanobiology*, jun 2020.
- 1113 [60] S.M. Hassanizadeh. Derivation of basic equations of mass transp. porous med., part 2. gen-  
1114 eralized darcy’s and fick’s laws. *Adv. Water Resour.*, 9:207–222, 1986.
- 1115 [61] Gabriel Helmlinger, Paolo A. Netti, Hera C. Lichtenbeld, Robert J. Melder, and Rakesh K.  
1116 Jain. Solid stress inhibits the growth of multicellular tumor spheroids. *Nature Biotechnology*,  
1117 15(8):778–783, aug 1997.
- 1118 [62] M.H. Holmes and V.C. Mow. The nonlinear characteristics of soft gels and hydrated connec-  
1119 tive tissues in ultrafiltration. *Journal of biomechanics*, 23:1145–1156, 1990.

- 1120 [63] Quanzhong Huang, Guanhua Huang, and Hongbin Zhan. A finite element solution for the  
1121 fractional advection-dispersion equation. *Advances in Water Resources*, 31(12):1578–1589,  
1122 dec 2008.
- 1123 [64] J. D. Humphrey. Towards a theory of vascular growth and remodeling. In Holzapfel G.A.  
1124 and Ogden R.W., editors, *Mechanics of Biological Tissue*, pages 3–15. Springer-Verlag, 2006.
- 1125 [65] Ruben Interian, Reinaldo Rodríguez-Ramos, Fernando Valdés-Ravelo, Ariel Ramírez-Torres,  
1126 Celso Ribeiro, and Aura Conci. Tumor growth modelling by cellular automata. *Mathematics  
1127 and Mechanics of Complex Systems*, 5(3-4):239–259, oct 2017.
- 1128 [66] R.K. Jain, J.D. Martin, and T. Stylianopoulos. The role of mechanical forces in tumor growth  
1129 and therapy. *Annual Review of Biomedical Engineering*, 16:321–346, 2014.
- 1130 [67] Chongming Jiang, Chunyan Cui, Li Li, and Yuanzhi Shao. The anomalous diffusion of a  
1131 tumor invading with different surrounding tissues. *PLoS ONE*, 9(10):e109784, oct 2014.
- 1132 [68] Ansgar Jüngel and Ines Viktoria Stelzer. Entropy structure of a cross-diffusion tumor-growth  
1133 model. *Mathematical Models and Methods in Applied Sciences*, 22(07):1250009, may 2012.
- 1134 [69] M A Konerding, E Fait, and A Gaumann. 3d microvascular architecture of pre-cancerous  
1135 lesions and invasive carcinomas of the colon. *British Journal of Cancer*, 84(10):1354–1362,  
1136 2001.
- 1137 [70] M. Köpf, C. Corinth, O. Haferkamp, and T.F. Nonnenmacher. Anomalous diffusion of water  
1138 in biological tissues. *Biophysical Journal*, 70(6):2950–2958, jun 1996.
- 1139 [71] R. Krishna and J.A. Wesselingh. The maxwell-stefan approach to mass transfer. *Chemical  
1140 Engineering Science*, 52(6):861–911, mar 1996.
- 1141 [72] E. Kröner. Elasticity theory of materials with long range cohesive forces. *International  
1142 Journal of Solids and Structures*, 3(5):731–742, sep 1967.
- 1143 [73] Ellen Kuhl. Growing matter: A review of growth in living systems. *J. Mech. Behav. Biomed.  
1144 Mater.*, 29:529–543, jan 2014.
- 1145 [74] Daniel J. Lacks. Tortuosity and anomalous diffusion in the neuromuscular junction. *Physical  
1146 Review E*, 77(4), apr 2008.
- 1147 [75] E. K. Lenzi, H. V. Ribeiro, A. A. Tateishi, R. S. Zola, and L. R. Evangelista. Anomalous  
1148 diffusion and transport in heterogeneous systems separated by a membrane. *Proceedings of  
1149 the Royal Society A: Mathematical, Physical and Engineering Sciences*, 472(2195):20160502,  
1150 nov 2016.
- 1151 [76] V.E. Lynch, B.A. Carreras, D. del Castillo-Negrete, K.M. Ferreira-Mejias, and H.R. Hicks.  
1152 Numerical methods for the solution of partial differential equations of fractional order. *Journal  
1153 of Computational Physics*, 192(2):406–421, dec 2003.
- 1154 [77] P. Macklin, Vittorio Cristini, and John Lowengrub. Biological background. In *Multiscale  
1155 Modeling of Cancer*, pages 8–23. Cambridge University Press, 2010.

- 1156 [78] Paul Macklin, Steven McDougall, Alexander R. A. Anderson, Mark A. J. Chaplain, Vittorio  
1157 Cristini, and John Lowengrub. Multiscale modelling and nonlinear simulation of vascular  
1158 tumour growth. *Journal of Mathematical Biology*, 58(4-5):765–798, sep 2009.
- 1159 [79] J.E. Marsden and T.J.R. Hughes. *Mathematical Foundations of Elasticity*. Dover Publica-  
1160 tions, Inc., Mineola, New York, 1983.
- 1161 [80] P. Mascheroni, M. Carfagna, A. Grillo, D.P. Boso, and B.A. Schrefler. An avascular tumor  
1162 growth model based on porous media mechanics and evolving natural states. *Mathematics  
1163 and Mechanics of Solids*, 23(4):686–712, jun 2018.
- 1164 [81] P. Mascheroni, C. Stigliano, M. Carfagna, D.P. Boso, L. Preziosi, P. Decuzzi, and B.A.  
1165 Schrefler. Predicting the growth of glioblastoma multiforme spheroids using a multiphase  
1166 porous media model. *Biomech. Model. Mechanobiol.*, 15(5):1215–1228, jan 2016.
- 1167 [82] Mark M. Meerschaert, Jeff Mortensen, and Stephen W. Wheatcraft. Fractional vector calculus  
1168 for fractional advection–dispersion. *Physica A: Statistical Mechanics and its Applications*,  
1169 367:181–190, jul 2006.
- 1170 [83] Mark M. Meerschaert and Charles Tadjeran. Finite difference approximations for two-sided  
1171 space-fractional partial differential equations. *Applied Numerical Mathematics*, 56(1):80–90,  
1172 jan 2006.
- 1173 [84] Ralf Metzler and Joseph Klafter. The random walk’s guide to anomalous diffusion: a frac-  
1174 tional dynamics approach. *Physics Reports*, 339(1):1–77, dec 2000.
- 1175 [85] M.V. Mićunović. *Thermomechanics of Viscoplasticity*. Springer New York, 2009.
- 1176 [86] Shlomo P. Neuman and Daniel M. Tartakovsky. Perspective on theories of non-fickian trans-  
1177 port in heterogeneous media. *Advances in Water Resources*, 32(5):670–680, may 2009.
- 1178 [87] K. Nishimoto. *Fractional Calculus: Integrations and Differentiations of Arbitrary Order*.  
1179 University of New Haven Press, 1989.
- 1180 [88] Keith B. Oldham and Jerome Spanier. *The Fractional Calculus. Theory and Applications of  
1181 Differentiation and Integration to Arbitrary Order*. Elsevier Science, 1974.
- 1182 [89] P. Paradisi, R. Cesari, F. Mainardi, A. Maurizi, and F. Tampieri. A generalized fick’s law to  
1183 describe non-local transport effects. *Physics and Chemistry of the Earth, Part B: Hydrology,  
1184 Oceans and Atmosphere*, 26(4):275–279, jan 2001.
- 1185 [90] R. Penta and D. Ambrosi. The role of the microvascular tortuosity in tumor transport  
1186 phenomena. *Journal of Theoretical Biology*, 364:80–97, jan 2015.
- 1187 [91] Raimondo Penta, Laura Miller, Alfio Grillo, Ariel Ramírez-Torres, Pietro Mascheroni, and  
1188 Reinaldo Rodríguez-Ramos. Porosity and diffusion in biological tissues. recent advances and  
1189 further perspectives. In *Constitutive Modelling of Solid Continua*, pages 311–356. Springer  
1190 International Publishing, nov 2020.

- 1191 [92] Igor Podlubny. *Fractional Differential Equations: An Introduction to Fractional Derivatives,*  
1192 *Fractional Differential Equations, to Methods of Their Solution and Some of Their Applica-*  
1193 *tions (ISSN Book 198).* Academic Press, 1998.
- 1194 [93] Adrien Poulenard and Maks Ovsjanikov. Multi-directional geodesic neural networks via equiv-  
1195 ariant convolution. *ACM Transactions on Graphics*, 37(6):1–14, dec 2018.
- 1196 [94] S. Preston and M. Elzanowski. Material uniformity and the concept of the stress space. In  
1197 Bettina Albers, editor, *Continuous Media with Microstructure*, pages 91–101. Springer-Verlag  
1198 Berlin Heidelberg, 1 edition, 2010.
- 1199 [95] L. Preziosi and G. Vitale. A multiphase model of tumor and tissue growth including cell  
1200 adhesion and plastic reorganization. *Math. Models Methods Appl. Sci.*, 21(09):1901–1932,  
1201 sep 2011.
- 1202 [96] Ariel Ramírez-Torres, Salvatore Di Stefano, Alfio Grillo, Reinaldo Rodríguez-Ramos, José  
1203 Merodio, and Raimondo Penta. An asymptotic homogenization approach to the microstruc-  
1204 tural evolution of heterogeneous media. *International Journal of Non-Linear Mechanics*,  
1205 106:245–257, nov 2018.
- 1206 [97] Ariel Ramírez-Torres, Reinaldo Rodríguez-Ramos, Rainer Glüge, Julián Bravo-Castillero,  
1207 Raúl Guinovart-Díaz, and Rocío Rodríguez-Sanchez. Biomechanic approach of a growing  
1208 tumor. *Mechanics Research Communications*, 51:32–38, jul 2013.
- 1209 [98] E.K. Rodriguez, A. Hoger, and A.D. McCulloch. Stress-dependent finite growth in soft elastic  
1210 tissues. *J. Biomech.*, 27:455–467, 1994.
- 1211 [99] John Paul Roop. Computational aspects of FEM approximation of fractional advection  
1212 dispersion equations on bounded domains in  $\mathbb{R}^2$ . *Journal of Computational and Applied*  
1213 *Mathematics*, 193(1):243–268, aug 2006.
- 1214 [100] Tiina Roose, S. Jonathan Chapman, and Philip K. Maini. Mathematical models of avascular  
1215 tumor growth. *SIAM Review*, 49(2):179–208, jan 2007.
- 1216 [101] S. Di Stefano, A. Ramírez-Torres, R. Penta, and A. Grillo. Self-influenced growth through  
1217 evolving material inhomogeneities. *International Journal of Non-Linear Mechanics*, 106:174–  
1218 187, 2018.
- 1219 [102] S. Sadik and A. Yavari. On the origins of the idea of the multiplicative decomposition of the  
1220 deformation gradient. *Mathematics and Mechanics of Solids*, 22(4):771–772, oct 2017.
- 1221 [103] Sandro Salsa, Federico M. G. Vegni, Anna Zaretti, and Paolo Zunino. Elementi di analisi  
1222 funzionale. In *UNITEXT*, pages 259–324. Springer Milan, 2009.
- 1223 [104] S. G. Samko, A. A. Kilbas, and O. I. Marichev. *Fractional Integrals and Derivatives: Theory*  
1224 *and Applications.* Gordon and Breach Science Publishers, 1993.
- 1225 [105] A. Sapora, P. Cornetti, B. Chiaia, E. K. Lenzi, and L. R. Evangelista. Nonlocal diffusion  
1226 in porous media: A spatial fractional approach. *Journal of Engineering Mechanics*, 143(5),  
1227 may 2017.

- 1228 [106] Stefan C. Schonsheck, Bin Dong, and Rongjie Lai. Parallel transport convolution: A new  
1229 tool for convolutional neural networks on manifolds. *arXiv preprint*, 2018.
- 1230 [107] G Sciumè, S Shelton, W G Gray, C T Miller, F Hussain, M Ferrari, P Decuzzi, and B A Schre-  
1231 fler. A multiphase model for three-dimensional tumor growth. *New J. Phys.*, 15(1):015005,  
1232 jan 2013.
- 1233 [108] Mihir Sen and Eduardo Ramos. A spatially non-local model for flow in porous media. *Trans-  
1234 port in Porous Media*, 92(1):29–39, oct 2011.
- 1235 [109] S.L. Sobolev. Nonlocal diffusion models: Application to rapid solidification of binary mix-  
1236 tures. *International Journal of Heat and Mass Transfer*, 71:295–302, apr 2014.
- 1237 [110] T. Stylianopoulos, J.D. Martin, V.P. Chauhan, S.R. Jain, and et al. Causes, conse-  
1238 quences, and remedies for growth-induced solid stress in murine and human tumors. *PNAS*,  
1239 109(38):15101–15108, 2012.
- 1240 [111] T. Stylianopoulos, J.D. Martin, M. Snuderl, F. Mpekris, S.R. Jain, and R.K. Jain. Coevolu-  
1241 tion of solid stress and interstitial fluid pressure in tumors during progression: Implications  
1242 for vascular collapse. *Cancer Research*, 73(13):3833–3841, apr 2013.
- 1243 [112] V. E. Tarasov and G. M. Zaslavsky. Fractional dynamics of systems with long-range interac-  
1244 tion. *Communications in Nonlinear Science and Numerical Simulation*, 11(8):885–898, dec  
1245 2006.
- 1246 [113] Vasily E. Tarasov. Fractional vector calculus and fractional maxwell’s equations. *Annals of  
1247 Physics*, 323(11):2756–2778, nov 2008.
- 1248 [114] A. Tomic, A. Grillo, and S. Federico. Poroelastic materials reinforced by statistically oriented  
1249 fibres — numerical implementation and application to articular cartilage. *IMA J. Appl.  
1250 Math.*, 79:1027–1059, 2014.
- 1251 [115] P. R. Wills, D. J. Scott, and D. J. Winzor. Thermodynamics and thermodynamic nonideality.  
1252 In G. C. K. Roberts, editor, *Encyclopedia of Biophysics*, pages 2583–2589. Springer, Berlin  
1253 Heidelberg, 2013.